The citrus flavonoid nobiletin confers protection from metabolic dysregulation in high-fat-fed mice independent of AMPK

Nadya M. Morrow,*,† Amy C. Burke,*,† Joshua P. Samsoondar,*,†,§ Kyle E. Seigel,*,† Andrew Wang,*,† Dawn E. Telford,*,§ Brian G. Sutherland,* Conor O'Dwyer, Gregory R. Steinberg,†† Morgan D. Fullerton,** and Murray W. Huff[1],*,†,§**

Molecular Medicine, Robarts Research Institute,* and Departments of Biochemistry† and Medicine,§ University of Western Ontario, London, Ontario, Canada N6A 5B7; Department of Biochemistry, Microbiology, and Immunology,** Ottawa Institute of Systems Biology, University of Ottawa, Ottawa, Ontario, Canada K1H 8M5; and Division of Endocrinology and Metabolism,†† Department of Medicine, McMaster University, Hamilton, Ontario, Canada L8S 4K1

ORCID ID: 0000-0002-7221-306X (M.D.F.)

Abstract Obesity, dyslipidemia, and insulin resistance, the increasingly common metabolic syndrome, are risk factors for CVD and type 2 diabetes that warrant novel therapeutic interventions. The flavonoid nobiletin displays potent lipid-lowering and insulin-sensitizing properties in mice with metabolic dysfunction. However, the mechanisms by which nobiletin mediates metabolic protection are not clearly established. The central role of AMP-activated protein kinase (AMPK) as an energy sensor suggests that AMPK is a target of nobiletin. We tested the hypothesis that metabolic protection by nobiletin required phosphorylation of AMPK and acetyl-CoA carboxylase (ACC) in mouse hepatocytes, in mice deficient in hepatic AMPK (*Ampkβ1*$^{-/-}$), in mice incapable of inhibitory phosphorylation of ACC (*AccDKI*), and in mice with adipocyte-specific AMPK deficiency (*iβ1β2AKO*). We fed mice a high-fat/high-cholesterol diet with or without nobiletin. Nobiletin increased phosphorylation of AMPK and ACC in primary mouse hepatocytes, which was associated with increased FA oxidation and attenuated FA synthesis. Despite loss of ACC phosphorylation in *Ampkβ1*$^{-/-}$ hepatocytes, nobiletin suppressed FA synthesis and enhanced FA oxidation. Acute injection of nobiletin into mice did not increase phosphorylation of either AMPK or ACC in liver. In mice fed a high-fat diet, nobiletin robustly prevented obesity, hepatic steatosis, dyslipidemia, and insulin resistance, and it improved energy expenditure in *Ampkβ1*$^{-/-}$, *AccDKI*, and *iβ1β2AKO* mice to the same extent as in WT controls. Thus, the beneficial metabolic effects of nobiletin in vivo are conferred independently of hepatic or adipocyte AMPK activation. These studies further underscore the therapeutic potential of nobiletin and begin to clarify possible mechanisms.—Morrow, N. M., A. C. Burke, J. P. Samsoondar, K. E. Seigel, A. Wang, D. E. Telford, B. G. Sutherland, C. O'Dwyer, G. R. Steinberg, M. D. Fullerton, and M. W. Huff. **The citrus flavonoid nobiletin confers protection from metabolic dysregulation in high-fat-fed mice independent of AMPK. *J. Lipid Res.* 2020.** 61: **387–402.**

Supplementary key words adenosine monophosphate-activated protein kinase • obesity • steatohepatitis • lipogenesis • fatty acid oxidation • insulin resistance • hypolipidemic drugs

Obesity, dyslipidemia, and insulin resistance are characteristic features of the metabolic syndrome, which is a clustering of risk factors for CVD and type 2 diabetes (1). These metabolic complications are increasing in prevalence, indicating a need for novel therapeutic interventions (2). Flavonoids are polyphenolic plant-derived metabolites that have been identified as potential therapeutic agents (3).

This work was supported by Canadian Institutes of Health Research Grant MOP-126045 and Heart and Stroke Foundation of Canada Grant G-14-0006179 to M.W.H. M.D.F. is supported by Canadian Institutes of Health Research Grant PJT148634 and New Investigator Award MSH141981. G.R.S. is supported by Canada Research Chairs, the J. Bruce Duncan Endowed Chair in Metabolic Diseases, Canadian Institutes of Health Research Program Grant 201709FDN-CEBA-116200, and a Diabetes Canada Program Grant. A.C.B. was supported by Diabetes Canada Doctoral Research Grant DS-3-14-4588-AB. The authors declare that they have no conflicts of interest with the contents of this article.

Manuscript received 20 November 2019 and in revised form 16 January 2020.

Published, JLR Papers in Press, January 21, 2020
DOI https://doi.org/10.1194/jlr.RA119000542

Abbreviations: ACC, acetyl-CoA carboxylase; AMPK, AMP-activated protein kinase; AUC, area under the curve; BAT, brown adipose tissue; Cpt, carnitine palmitoyltransferase; CE, cholesteryl ester; eWAT, epididymal white adipose tissue; FC, free cholesterol; FPLC, fast-protein LC; HFHC, high-fat/high-cholesterol; iGTT, incremental glucose tolerance test; ITT, insulin tolerance test; iWAT, inguinal white adipose tissue; Ldlr, LDL receptor; pACC, phosphorylated acetyl-CoA carboxylase; pAMPK, phosphorylated AMP-activated protein kinase; RER, respiratory exchange ratio; ROR, retinoic acid receptor-related orphan receptor; TC, total cholesterol; TG, triglyceride; WAT, white adipose tissue.

[1] To whom correspondence should be addressed.
e-mail: mhuff@uwo.ca

[S] The online version of this article (available at https://www.jlr.org) contains a supplement.

Citrus flavonoids, including naringenin and nobiletin, have been documented for their bioactive utility, including attenuating risk factors for CVD and type 2 diabetes (3–8). In mouse models of the metabolic syndrome, nobiletin markedly attenuated metabolic dysregulation and slowed the development of atherosclerosis (7, 9–11). Although the bioavailability is low, nobiletin accumulates in the liver with lesser amounts in adipose tissue and muscle of mice, indicating that the liver is a primary target (3, 7).

Nobiletin potently reduced apolipoprotein B secretion from HepG2 cells, which was associated with reduced activity of microsomal triglyceride (TG) transfer protein and acyl-CoA:diacylglycerol acyltransferase and increased expression of LDL receptors (*Ldlr*s) (7). In C57BL/6 or $Ldlr^{-/-}$ mice fed a high-fat diet, supplementation with nobiletin prevented weight gain, adiposity, hyperlipidemia, hepatic steatosis, and insulin resistance, without effect on caloric intake (7). Regression studies in $Ldlr^{-/-}$ mice revealed that intervention by nobiletin reversed existing obesity and decreased adipocyte size and number, improved hyperlipidemia, insulin sensitivity, and hepatic steatosis, and enhanced energy expenditure (10). In the liver, nobiletin increased the gene expression of hepatic PPARγ co-activator 1α (*Pgc1a*) and carnitine palmitoyltransferase (*Cpt*) *1a* leading to increased hepatic FA oxidation (7). In addition, nobiletin decreased the expression of hepatic *Srebf1c* accompanied by suppression of hepatic FA synthesis (7). These regulatory effects presumably account for nobiletin's capacity to attenuate hepatic TG accumulation and prevent metabolic dysregulation. However, the specific upstream mechanisms by which nobiletin mediates these effects remain elusive.

AMP-activated protein kinase (AMPK) is a αβγ heterotrimer central to the regulation of cellular energy homeostasis (12, 13). Multiple levels of hormonal, nutritional, and cytokine stimuli mediate the activation of AMPK in most tissues, leading to inhibition of anabolic processes and stimulation of ATP-generating catabolic processes (14, 15). Specifically, phosphorylation of the α catalytic subunit of AMPK at Thr172 results in inhibitory phosphorylation of acetyl-CoA carboxylase (ACC) 1 at Ser79 and ACC2 at Ser212, which decreases the conversion of acetyl-CoA to malonyl-CoA, the rate-limiting step in de novo FA synthesis (14). Malonyl-CoA also functions as an allosteric inhibitor of CPT1, a protein that facilitates the rate-limiting transport of FA into the mitochondria for FA oxidation (14). Thus, AMPK-mediated phosphorylation of ACC not only suppresses FA synthesis but also relieves the repression of FA oxidation by malonyl-CoA. AMPK indirectly upregulates FA oxidation by increasing mitochondrial biogenesis through PGC1α (15). AMPK also mediates suppression of FAS through phosphorylation and inactivation of SREBP-1c (16).

A variety of drugs, xenobiotics, polyphenols, and flavonoids activate AMPK, including A-769662, salicylate, metformin, berberine, quercetin, resveratrol, and genistein (17–19). Enhanced phosphorylation of AMPK and ACC in HepG2 cells or primary mouse hepatocytes by metformin, A-769662, or resveratrol increased FA oxidation, decreased FA synthesis, and reduced cellular TG (18, 20), effects similar to HepG2 cells exposed to nobiletin (7). Recent studies in cultured HepG2 cells reported that nobiletin blunted palmitate-induced lipogenesis and inhibited the protein expressions of SREBP-1c and FAS via phosphorylation of AMPK and ACC (21, 22). Also, the metabolic protection associated with nobiletin treatment in mouse models is similar to the effects of pharmacological activation of AMPK, as observed with the PPARδ agonist GW1516, metformin, salicylate, and resveratrol (23–25). Taken together, these observations suggest that AMPK activation may be a target of nobiletin. One of the objectives of the present study was to determine the requirement of nobiletin to activate AMPK and improve lipid metabolism in cultured hepatocytes, in mouse liver following acute nobiletin administration and in chronically treated mice with or without genetic inactivation of hepatic AMPK ($Ampk\beta1^{-/-}$) or phosphorylation-defective ACC1 and -2 (*AccDKI*).

Current understanding of the role of AMPK in adipose tissue is primarily based on studies conducted in cultured cells (26–28) and in mice lacking single subunits of AMPK that retain significant residual AMPK activity (29–31). Recently, Motillo et al. (32) reported that inducible deletion of both AMPKβ1 and -β2 in mouse adipocytes (*iβ1β2AKO*) inhibited the ability of β-adrenergic agonists to stimulate browning of white adipose tissue (WAT) and amplified diet-induced hepatic steatosis and insulin resistance. In cultured 3T3-L1 white adipocytes, nobiletin was shown to stimulate browning (33), reduce cellular TG content, and inhibit adipogenesis through phosphorylation of AMPK (33–35). Therefore, we hypothesized that activation of adipocyte AMPK was an integral part of nobiletin's mechanism of action, and that adipocyte-specific AMPK deficiency would compromise metabolic protection mediated by nobiletin.

In primary C57BL/6 (WT) hepatocytes, nobiletin increased the phosphorylation of AMPK and ACC, which was associated with suppressed FA synthesis and increased FA oxidation. Despite the loss of ACC phosphorylation in $Ampk\beta1^{-/-}$ hepatocytes, nobiletin was still able to suppress FA synthesis and enhance FA oxidation. Acute injection of nobiletin into mice did not increase phosphorylation of either AMPK or ACC in the liver. In mice fed a high-fat diet, nobiletin supplementation robustly prevented metabolic dysregulation in $Ampk\beta1^{-/-}$, *AccDKI*, and *iβ1β2AKO* mice to the same extent as in WT controls. Thus, metabolic protection by nobiletin in vivo is conferred independently of hepatic or adipocyte AMPK.

MATERIALS AND METHODS

Animals and diets

Male $Ldlr^{-/-}$ mice on a C57BL/6J background (Jackson Laboratory, Bar Harbor, ME) were bred in-house. Male $Ampk\beta1^{-/-}$ mice on a C57BL/6J background and littermate controls were generated as described previously (30). $Ampk\beta1^{-/-}$ mice have a 90% reduction in liver AMPK activity compared with WT mice. Female *Acc1*-S79A and *Acc2*-S212A knock-in mutation mice (*AccDKI*) on a C57BL/6J background and littermate controls were generated as previously described (36). Male mice (C57BL/6J) with inducible deficiency of adipocyte Ampkβ1and -β2 (*iβ1β2AKO*) along with

littermate controls were generated by crossing mice (C57BL/6J) containing an adiponectin B6N promoter-controlled and tamoxifen-inducible Cre recombinase (AdipoQ-CreERT2) with mice deficient for the β1 and β2 AMPK subunits ($Ampk\beta1^{flox/flox}\beta2^{flox/flox}$) as previously described (32). At 8 weeks of age, $Ampk\beta1^{flox/flox}\beta2^{flox/flox}$ *CreERT2* and $Ampk\beta1^{flox/flox}\beta2^{flox/flox}$ (control) mice were administered 0.1 g/kg body weight tamoxifen (Cayman Chemical) by daily oral gavage for 5 days to induce deletion of adipocyte AMPK (32) and continued on a standard chow diet (14% kcal fat; diet #T.8604; Envigo, Madison, WI) for 3 weeks until the start of experiments. At 10–12 weeks of age, all mice were fed ad libitum for 12 or 18 weeks (n = 5–10 per group) with either a high-fat/high-cholesterol (HFHC) diet (42% kcal fat, 0.2% w/w cholesterol; diet #TD.09268; Envigo) or a HFHC diet supplemented with 0.3% w/w nobiletin (R&S PharmChem, Hangzhou City, China). Taste aversion with nobiletin was mitigated by slowly increasing the flavonoid dose over week 1 to prevent suppression of food intake. All mice were housed in pairs in standard cages at 23°C on a 12 h light/dark cycle. Food consumption and body weights were recorded weekly. Caloric consumption was calculated as the weight of food consumed per day (grams) multiplied by the caloric content of the diet (HFHC diet: 4.5 kcal/g). All experiments followed the Canadian Guide for the Care and Use of Laboratory Animals and were approved by the University of Western Ontario Animal Care Committee (protocol #AUP-2016-057).

Cell culture

The human hepatocellular carcinoma cell line, HepG2, was obtained from American Type Culture Collection (Manassas, VA). Cells were maintained in monolayer in DMEM supplemented with 10% FBS, 0.25 μg/ml Fungizone (Life Technologies, Burlington, Ontario, Canada), 10 U/ml penicillin (Life Technologies), and 10 μg/ml streptomycin (Life Technologies) (7). For experiments, cells were cultured to ∼80% confluence in 6-well (35 mm) plates (Falcon, Mississauga, Ontario, Canada). Prior to the experiment, cells were quiesced overnight in serum-free DMEM, and for experiments, treatments were administered in serum-free DMEM for up to 1 h. Cells were incubated in DMEM plus DMSO alone or with nobiletin (10 μM), resveratrol (10 μM; Sigma-Aldrich, Oakville, Ontario, Canada), or metformin (2 mM; Calbiochem EMD Inc., Mississauga, Ontario, Canada), which were all dissolved and diluted in DMSO. Low- and high-glucose experiments refer to DMEM media containing 5.5 and 30 mM glucose, respectively. Incubation of cells in high glucose mimics hyperglycemia and insulin resistance and suppresses phosphorylation of AMPK (20).

Primary mouse hepatocytes were isolated from chow-fed C57BL/6 WT or $Ampk\beta1^{-/-}$ mice by the collagenase perfusion method as described previously (23). Experiments were performed the day following hepatocyte isolation. For AMPK and ACC phosphorylation experiments, hepatocytes were incubated for 0–1 h with either DMSO alone, nobiletin (2–100 μM), resveratrol (10 μM), metformin (2 mM), salicylate (3 mM; Sigma), or A-769662 (100 μM; Selleck Bio, Houston, TX), a synthetic activator of AMPK (18). For lipogenesis and FA-oxidation experiments, cells were washed with PBS and incubated in serum-free Medium 199. Lipogenesis was assessed by incubating cells for 4 h with serum-free Medium 199 containing [1-^{3}H]acetate (0.5 μCi/ml; Amersham Biosciences) and 0.5 mM unlabeled sodium acetate, with or without treatments. Subsequently, cells were washed twice with PBS prior to lipid extraction and for determination of [1-^{3}H]acetate incorporation into TG (23). For FA oxidation, cells were incubated for 4 h with serum-free Medium 199 containing [1-^{14}C] palmitic acid (0.5 μCi/ml; Amersham Biosciences) and 0.5 mM unlabeled palmitate, with or without treatments. FA oxidation was determined by measuring conversion of [1-^{14}C]palmitic acid into CO_2 and acid-soluble metabolites as described previously (36).

Blood and tissue collection

Mice were fasted for 6 h at the start of the light cycle prior to blood taking or euthanization. At the time of euthanization, animals were anesthetized with ketamine-xylazine [100 μg/g ketamine hydrochloride (Bioniche Animal Health Canada Inc., Belleville, Ontario, Canada) and 10 μg/g xylazine (Bayer Healthcare, Animal Health Division, Bayer Inc., Toronto, Ontario, Canada)]. Blood was collected via cardiac puncture in syringes containing 40 μl of 7% Na_2-EDTA. Blood was centrifuged at 16,000 *g* for 10 min at 4°C to separate plasma, which was stored at −20°C. Tissue dissections were performed via midline incision. A section of liver tissue was harvested by freeze-clamping (37) and stored at −80°C prior to analyses. Small pieces of epididymal white adipose tissue (eWAT) and inguinal white adipose tissue (iWAT) as well as brown adipose tissue (BAT) were fixed in 4% paraformaldehyde and paraffin embedded for histological analyses. The remaining liver, eWAT, iWAT, and BAT were removed, weighed, and snap-frozen in liquid N_2 and stored at −80°C.

Plasma measurements

Plasma TG and cholesterol were measured on a Cobas Mira S autoanalyzer (Roche Diagnostics) using calibrators and controls from Roche (6). Enzymatic reagents for TG (Roche; TGs/glycerol blanked, #11877771 216) and cholesterol (Roche Diagnostics; Cholesterol CHOD-PAP, #11491458-216) were used. Fresh-EDTA plasma (50 μl) was separated by fast-protein LC (FPLC) using an AKTA purifier and a Superose 6 column (5). An aliquot of each fraction was used to measure cholesterol and TGs enzymatically in both samples and standards on a microtiter plate with added enzymatic reagents [TG (Roche Diagnostics,TGs/glycerol blanked, #11877771 216) and total cholesterol (TC) (WAKO Diagnostics, Cholesterol E, CHOD-DAOS method, #439-17501)]. Glucose was measured in whole blood using the Bayer contour blood glucose monitoring system (Bayer Healthcare, Etobicoke, Ontario, Canada) (6). Plasma insulin was determined in EDTA-plasma samples (stored at −20°C) by a mouse-specific ELISA (Mouse Ultrasensitive ELISA, #80-INSMSU-E01; ALPCO Diagnostics, Salem, NH) (6).

Liver lipid analyses

Lipids from liver dissected free of fat and connective tissue and stored at −80°C were extracted as described previously (10). [Cholesteryl-1,2-^{3}H(N)]cholesteryl oleate (PerkinElmer, Guelph, Ontario, Canada; #NET746L) was added to assess recovery. Solvent from each sample was dried under N_2 and a 1% Triton X-100 solution in chloroform was added to solubilize lipids. Samples were dried under N_2, followed by the addition of deionized water and analyses using enzymatic reagents for TG, TC (see above for FPLC analyses), and free cholesterol (FC) [WAKO Diagnostics; FC (COD-DAOS) method, #435-35801]. Cholesteryl ester (CE) was determined as the difference between TC and FC.

Liver FA oxidation

Fresh liver (250 mg) was homogenized in 0.1 M phosphate buffer (pH 7.2) containing 0.25 M sucrose, 1 mM EDTA, 1 mM dithiothreitol, and 10 μl/ml of protease inhibitor (Sigma-Aldrich; #P8340) (6). Homogenates were centrifuged at 1,000 *g* at 4°C for 10 min. Supernatant (20 μl) was incubated for 30 min at 37°C with constant shaking in 0.1 M phosphate buffer (pH 7.2) containing 150 mM KCl, 10 mM HEPES, 5 mM Tris malonate, 10 mM $MgCl_2$, 1 mM carnitine, 5 mM ATP, and 2 μCi of [9,10-^{3}H(N)] palmitic acid (PerkinElmer; #NET043001MC) per 50 μM of unlabeled palmitic acid complexed with 0.15% FA-free BSA. Reactions were stopped with 200 μl of 0.6 N perchloric acid and unreacted FAs were extracted with hexanes. The ^3H_2O in the aqueous phase was measured by liquid scintillation counting (6).

Glucose and insulin tolerance tests

Glucose tolerance tests were performed following a 6 h fast by intraperitoneal injection with 15% glucose in 0.9% NaCl (1 g/kg body weight) (6). Blood samples for glucose analyses (glucometer) were taken up to 120 min postinjection. An insulin tolerance test (ITT) was conducted following a 5 h fast by intraperitoneal injection with insulin (0.6 IU/kg body weight; Novolin GE Toronto, Novo Nordisk, Cooksville, Ontario, Canada) (6). Blood samples for glucose analyses were obtained up to 60 min postinjection. Glucose tolerance was determined from the incremental change in blood glucose from baseline concentrations and insulin tolerance was determined from the percent change in blood glucose from baseline concentrations (10).

Metabolic cage studies

Energy expenditure, respiratory exchange ratio (RER), and ambulatory activity were assessed using the Comprehensive Laboratory Animal Monitoring System (CLAMS; Columbus Instruments, Columbus, OH) as described previously (10). Mice were housed in metabolic cages with free access to food and water and acclimatized for 48 h. For the subsequent 24 h, every 10 min, data on O_2 consumption (VO_2; milliliters per hour) and CO_2 production (VCO_2; milliliters per hour) were collected. The RER was derived from the ratio of VCO_2 to VO_2, and energy expenditure was determined as $(3.815 + 1.232 \times \text{RER}) \times VO_2$ and expressed as ANCOVA-adjusted energy expenditure in kilocalories per hour. ANCOVA adjustments to energy expenditure were made based on body weight, which allowed for the determination of differences in energy expenditure independent of group differences in body weight (10). Ambulatory activity was measured as infrared beam breaks in the X, Y, and Z axes per hour.

Activation of AMPK in vivo

Activation of AMPK in vivo was assessed in chow-fed WT, *Ampkβ1*$^{-/-}$, and *Ldlr*$^{-/-}$ mice following intraperitoneal injection of nobiletin or A-769662 as described previously (23, 38). Animals were fasted overnight (1900–0700), followed by free access to food (chow) at 0700 for 2 h. At 0900, chow was removed, and mice were injected intraperitoneally with vehicle (5% DMSO in PBS), 50 mg/kg nobiletin, or 30 mg/kg A-769662. Ninety minutes postinjection, the mice were anesthetized (described above) and euthanized. A section of liver tissue was harvested by freeze-clamping (37) and stored at −80°C prior to analyses. Blood was collected in syringes containing 80 μl of 7% Na_2-EDTA by cardiac puncture, and plasma was stored at −20°C.

Immunoblotting

Cell lysates from HepG2 cells or primary mouse hepatocytes were prepared using a minor modification of a previously described method (39, 40). Briefly, total cell or tissue lysates from snap-frozen freeze-clamped liver samples (∼50 mg) were prepared in lysis buffer [20 mM Tris (pH 7.4), 50 mM NaCl, 1 mM EDTA (pH 8.0), 1 mM EGTA (pH 8.0), 1% Triton X-100, 1 mM NaF] containing protease inhibitor cocktail (Sigma, St. Louis, MO) 1:100 and phosphatase inhibitor cocktail (Sigma) 1:100. Tissues were homogenized on ice using a tissue grinder and the lysate was obtained by centrifugation (11,300 *g*, 2 min, 4°C) and stored at −80°C. Proteins were separated by SDS-PAGE on 7.5% polyacrylamide gels (Bio-Rad) and transferred to Immobilon-FL PVDF membranes (EMD Millipore, Darmstadt, Germany). Membranes were probed using antibodies against phosphorylated and total AMPK and ACC as well as β-actin or GAPDH. Antibodies from Cell Signaling (Danvers, MA) were phosphorylated AMPK (pAMPK)α T172 #2531, AMPKα #2532, AMPKβ1/β2 #4150, phosphorylated ACC (pACC)ser79/212 #3661, ACC #3676, β-actin #5125, and GAPDH #97166. Antibodies from R&D Systems (Minneapolis, MN) were AMPKα #AF3197 and ACCα #MAB6898, and antibodies from Santa Cruz Biotechnology (Dallas, TX) were ACCβ #SC390522. Detection was performed with appropriate secondary antibodies from Cell Signaling (anti-rabbit IgG HRP-linked #7074 and anti-mouse rabbit IgG HRP-linked #7076) or from LI-COR Biosciences (Lincoln, NE) [IRDye® 680RD donkey anti-rabbit IgG (H+L) #925-68073, IRDye® 800CW donkey anti-goat IgG (H+L) #925-32214, IRDye® 680RD goat anti-mouse IgG (H+L) #926-68070, and IRDye® 800CW goat anti-rabbit IgG (H+L) #926-32211]. For blots using HRP-linked secondary antibodies, detection was determined using enhanced chemiluminescence reagent (Roche Diagnostics) and quantification was performed using an imaging densitometer (GS-700; Bio-Rad Laboratories, Mississauga, Ontario, Canada). For blots using LI-COR secondary antibodies, imaging and quantitation of immunoblots were performed using the LI-COR Odyssey Fc (LI-COR Biosciences) and the LI-COR Image Studio Software 5.0.

Gene expression

RNA was extracted from iWAT tissue using TriZol reagent and was reverse-transcribed to cDNA using previously published methods (6). PCR primers and TaqMan probes for *Ucp1*, *Cd137*, *Tbx1*, *Serca2b*, *Ampkb1*, *Ampkb2*, and *Ppia* were obtained from Life Technologies (Burlington, Ontario, Canada). mRNA expression of each gene was determined by quantitative real-time PCR on an ABI ViiA 7 detection system (Applied Biosystems, Streetsville, CA) using the standard curve method, as previously published (6). mRNA expression levels were normalized to the expression of *Ppia* (32).

Histology

Samples of iWAT, eWAT, and BAT were collected, weighed, fixed in 4% paraformaldehyde for 24 h, processed, embedded in paraffin, and sectioned (5 μm) on a Micron HM335E microtome (Thermo Fisher Scientific). Sections were stained with H&E and photomicrographs were obtained using an Olympus BX51 microscope (Olympus Canada, Richmond Hill, Ontario, Canada). Quantification of adipocyte area and the number of cells per field of view (>100 cells/mouse) was performed using ImageJ 1.50 software (National Institutes of Health) and the Adiposoft plugin (10). Total adipocyte number was determined by multiplying the average number of cells per field of view by the tissue weight.

Statistical analysis

Data are presented as mean ± SEM. Statistical analyses were performed using GraphPad Prism 8. A one-way ANOVA with post hoc Tukey's test was used to test for differences between groups, except in the case of parameters measured over time where a two-way repeated measures ANOVA with post hoc Tukey's test was used. Significance thresholds were $P < 0.05$. Different letters indicate significant differences. A Student's *t*-test was used to assess differences in ANCOVA-adjusted energy expenditure; an asterisk indicates significant differences ($P < 0.05$).

RESULTS

Nobiletin activates AMPK in HepG2 cells

Previous studies have shown that polyphenols, such as nobiletin activate AMPK in cultured HepG2 cells (20–22). In the present study, we incubated HepG2 cells with nobiletin and the positive controls, resveratrol and metformin. Nobiletin increased AMPK phosphorylation (pAMPK)

1.8-fold, similar to the activation by resveratrol (2.0-fold) and metformin (2.2-fold) (**Fig. 1A**). Resveratrol and metformin have also been shown to reverse the decrease in AMPK and ACC phosphorylation induced by incubation of HepG2 cells in elevated glucose (30 mM), a condition that mimics cellular insulin resistance (20). Incubation of HepG2 cells with high glucose suppressed the phosphorylation of AMPK and ACC. Addition of nobiletin reversed

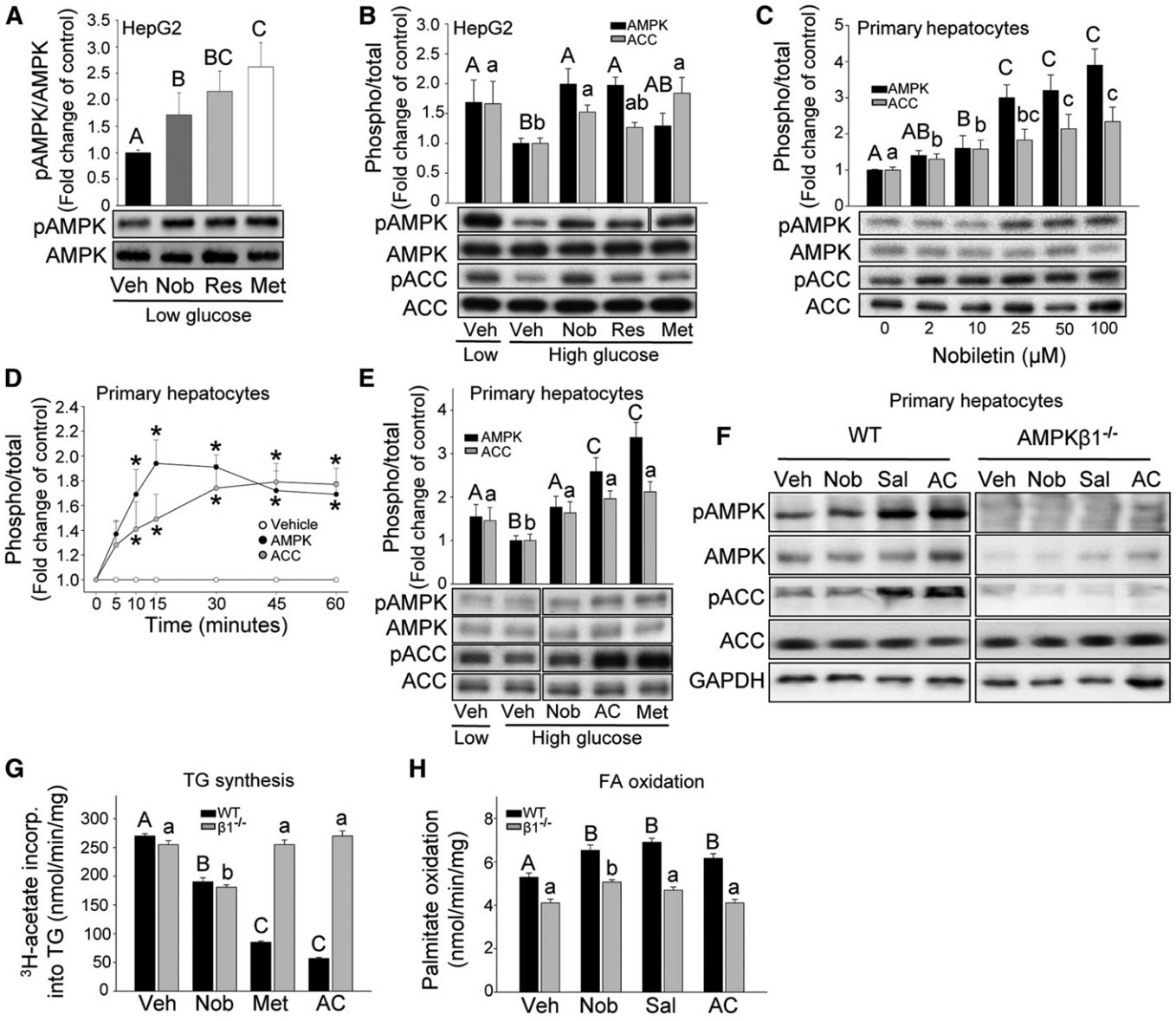

Fig. 1. Nobiletin increases the phosphorylation of AMPK and ACC in HepG2 cells and primary mouse hepatocytes, but regulates lipid metabolism similarly in *Ampkβ1*$^{-/-}$ and WT hepatocytes. A, B: HepG2 cells incubated with vehicle (Veh), nobiletin (Nob; 10 μM), resveratrol (Res; 10 μM), and metformin (Met; 2 mM) for 1 h in low glucose (5.5 mM) (A, B) or high glucose (30 mM) (B) media. Representative immunoblots of phosphorylated (p)AMPK, AMPK, pACC, or ACC and quantitation (n = 4–5) expressed as fold change compared with Veh low glucose (A) or Veh high glucose (B) controls. C, D: Primary hepatocytes from WT mice incubated in low glucose with nobiletin (0–100 μM) for 1 h (C) or nobiletin (25 μM) from 0 to 60 min (D). Representative immunoblots for pAMPK, AMPK, pACC, and ACC (C) and mean density quantitation (C,,D) for n = 4–5, expressed as the fold change in the ratio of phosphorylated to total, compared with Veh. E: WT hepatocytes incubated with vehicle, nobiletin (25 μM), A-769662 (AC) (100 μM), or metformin (2 mM) for 1 h in low (5.5 mM) or high (30 mM) glucose. Representative immunoblot and mean density quantitation for n = 4, expressed as fold change in the ratio of phosphorylated to total, compared with vehicle high glucose. F: Representative immunoblot of cell lysates from WT and *Ampkβ1*$^{-/-}$ hepatocytes incubated with vehicle, nobiletin (25 μM), salicylate (3 mM), or A-769662 (100 μM) in low glucose for 1 h and probed for pAMPK, AMPK, pACC, and ACC. Immunoblots shown are from the same gel; for some blots, lanes were reordered for consistency. Different upper case letters indicate significant differences among treatments for pAMPK/AMPK and different lowercase letters indicate significant differences among treatments for pACC/ACC, analyzed by ANOVA with post hoc Tukey's test ($P < 0.05$). Asterisks (*) indicate a significant difference from vehicle, analyzed by Student's paired *t*-test ($P < 0.05$). G: TG synthesis in primary hepatocytes from WT or *Ampkβ1*$^{-/-}$ mice incubated with vehicle, nobiletin (Nob; 25 μM), metformin (Met; 2 mM), or A-769662 (AC; 100 μM). B: FA oxidation in primary hepatocytes from WT or *Ampkβ1*$^{-/-}$ mice incubated with vehicle, nobiletin (25 μM), salicylate (Sal; 3 mM), or A-769662 (100 μM). Different upper case letters indicate statistical differences for WT mice and different lowercase letters indicate statistical differences for *Ampkβ1*$^{-/-}$ mice.

this effect by stimulating AMPK phosphorylation (2-fold) to levels observed with low glucose (Fig. 1B). Increases were also observed for resveratrol (2.0-fold) and metformin (1.4-fold). ACC phosphorylation was suppressed by high glucose (−38%), which was reversed by nobiletin (1.5-fold), resveratrol (1.3-fold), and metformin (1.8-fold).

Nobiletin reduces lipogenesis and increases FA oxidation independent of AMPK in primary mouse hepatocytes

As the metabolic protection by nobiletin has been demonstrated in mouse models, we next examined the ability of nobiletin to increase the phosphorylation of AMPK and ACC in primary mouse hepatocytes from C57BL/6J mice. Initial dose-response studies in isolated hepatocytes cultured in normal glucose media showed that nobiletin increased pAMPK (2-fold) and increased pACC (2-fold) at concentrations ⩾10 μM (Fig. 1C). Time-course experiments demonstrated that nobiletin at 25 μM maximally increased pAMPK by 15 min and pACC from 30 to 60 min (Fig. 1D). Incubation of mouse hepatocytes in high glucose, with or without nobiletin (25 μM) for 1 h, demonstrated that nobiletin reversed the glucose-suppressed phosphorylation of AMPK (1.8-fold) and ACC (1.7-fold) (Fig. 1E). The positive controls, A-769662, a synthetic AMPK activator, and metformin, increased the high glucose-suppressed pAMPK by 2.5-fold and pACC by 2.0-fold (Fig. 1E).

The functional significance of AMPK activation by nobiletin was assessed in hepatocytes isolated from *Ampkβ1*$^{-/-}$ and WT mice. The ability of nobiletin, A769662, and salicylate to increase the phosphorylation of ACC was lost in *Ampkβ1*$^{-/-}$ hepatocytes, indicating that ACC phosphorylation was dependent on AMPK (Fig. 1F). However, nobiletin suppressed lipogenesis to the same extent in both WT (−31%) and *Ampkβ1*$^{-/-}$ (−29%) hepatocytes (Fig. 1G). In contrast, lipogenesis was inhibited by metformin (−69%) and A-769662 (−77%) in WT hepatocytes but not in *Ampkβ1*$^{-/-}$ hepatocytes. Nobiletin increased palmitate oxidation similarly (24%) in hepatocytes from both WT and *Ampkβ1*$^{-/-}$ mice, whereas salicylate and A-769662 increased palmitate oxidation in WT hepatocytes (32% and 18%, respectively) but had no effect in *Ampkβ1*$^{-/-}$ hepatocytes (Fig. 1H). This suggests that nobiletin's ability to decrease lipogenesis and stimulate FA oxidation in primary hepatocytes is independent of AMPKβ1 or ACC phosphorylation.

Nobiletin does not acutely activate AMPK in vivo

Acute administration of salicylate and A-769662 to mice has been shown to activate hepatic AMPK and ACC (38). The ability of nobiletin to acutely activate AMPK in vivo was evaluated using a fasting, feeding, intraperitoneal injection, and refasting protocol (23) in chow-fed C57BL/6 WT, chow-fed *Ampkβ1*$^{-/-}$, and HFHC diet-fed *Ldlr*$^{-/-}$ mice. In livers isolated 90 min after the injection of nobiletin, the phosphorylation of AMPK or ACC was not affected in chow-fed WT mice, chow-fed *Ampkβ1*$^{-/-}$ mice, or HFHC diet-fed *Ldlr*$^{-/-}$ mice (supplemental Fig. S1A–E). Under the same conditions, A-769662 had no effect on hepatic ACC phosphorylation in chow-fed *Ampkβ1*$^{-/-}$ mice, but increased phosphorylation of AMPK and ACC in the other two groups of mice (supplemental Fig. S1A–E). This suggests that nobiletin's ability to confer metabolic protection is not through acute activation of AMPK.

Nobiletin prevents metabolic dysregulation in HFHC diet-fed *Ampkβ1*$^{-/-}$ mice

Treatment of mice with nobiletin increases energy expenditure, induces weight loss, lowers insulin resistance, and decreases liver and plasma lipids (7), effects that are analogous to pharmacological activation of AMPK (13, 18, 23–25). To investigate whether metabolic protection by nobiletin was mediated through AMPKβ1, starting at 10 weeks of age, WT and *Ampkβ1*$^{-/-}$ littermates were fed a HFHC diet with or without nobiletin for 12 weeks. *Ampkβ1*$^{-/-}$ mice have an ∼90% reduction in liver AMPK activity (30), and, as anticipated, levels of AMPK, pAMPK, and pACC in the livers of *Ampkβ1*$^{-/-}$ mice were markedly reduced compared with WT mice (**Fig. 2A**). Mice lacking hepatic AMPK gained a similar amount of weight in response to the HFHC diet as the WT mice (Fig. 2B). Nobiletin supplementation prevented HFHC diet-induced weight gain in *Ampkβ1*$^{-/-}$ mice to the same extent as in WT mice. Caloric intake was unaffected by nobiletin in both genotypes (Fig. 2C). The HFHC diet increased eWAT depots to similar levels in *Ampkβ1*$^{-/-}$ and WT mice (Fig. 2D). The striking reduction in eWAT in nobiletin-supplemented mice (∼56%) was similar in each genotype (Fig. 2D).

Energy expenditure and RER did not differ between HFHC diet-fed *Ampkβ1*$^{-/-}$ and WT mice (Fig. 2E, F). Nobiletin induced an ∼20% increase in ANCOVA-adjusted energy expenditure in both WT and *Ampkβ1*$^{-/-}$ mice (Fig. 2E). RER and activity levels were unaffected by genotype or nobiletin treatment (Fig. 2F, G). In HFHC diet-fed mice, plasma concentrations of TC and TG were not different between *Ampkβ1*$^{-/-}$ and WT mice (Fig. 2H, I). Nobiletin decreased plasma cholesterol in both *Ampkβ1*$^{-/-}$ (−45%) and WT (−30%) mice. Nobiletin lowered plasma TG levels similarly (∼26%) in both genotypes. FPLC profiles of plasma lipoproteins indicated that the nobiletin-induced reductions in LDL-C (∼60%) were similar for *Ampkβ1*$^{-/-}$ and WT mice (Fig. 2J, K). Nobiletin had no effect on HDL-C in controls, but decreased HDL-C by 46% in *Ampkβ1*$^{-/-}$ mice (Fig. 2L).

There was no difference in fasting blood glucose or glucose tolerance between *Ampkβ1*$^{-/-}$ and WT mice (**Fig. 3A**, B). Addition of nobiletin to the HFHC diet decreased fasting blood glucose (−17%) and improved glucose tolerance (46%) in WT mice. In *Ampkβ1*$^{-/-}$ mice, nobiletin also decreased fasting blood glucose (−21%) and improved glucose tolerance (33%), although the decrease in incremental glucose tolerance test (iGTT) area under the curve (AUC) in *Ampkβ1*$^{-/-}$ mice did not reach statistical significance (Fig. 3C). Insulin resistance was similar between *Ampkβ1*$^{-/-}$ and WT mice (Fig. 3E, F), and nobiletin decreased plasma insulin (∼80%) and improved insulin tolerance AUC (∼29%) to a similar degree in both *Ampkβ1*$^{-/-}$ and WT mice. Nobiletin induced striking reductions in hepatic TG and CE in both genotypes, although the extent of reduction was greater in control mice (Fig. 3G, H).

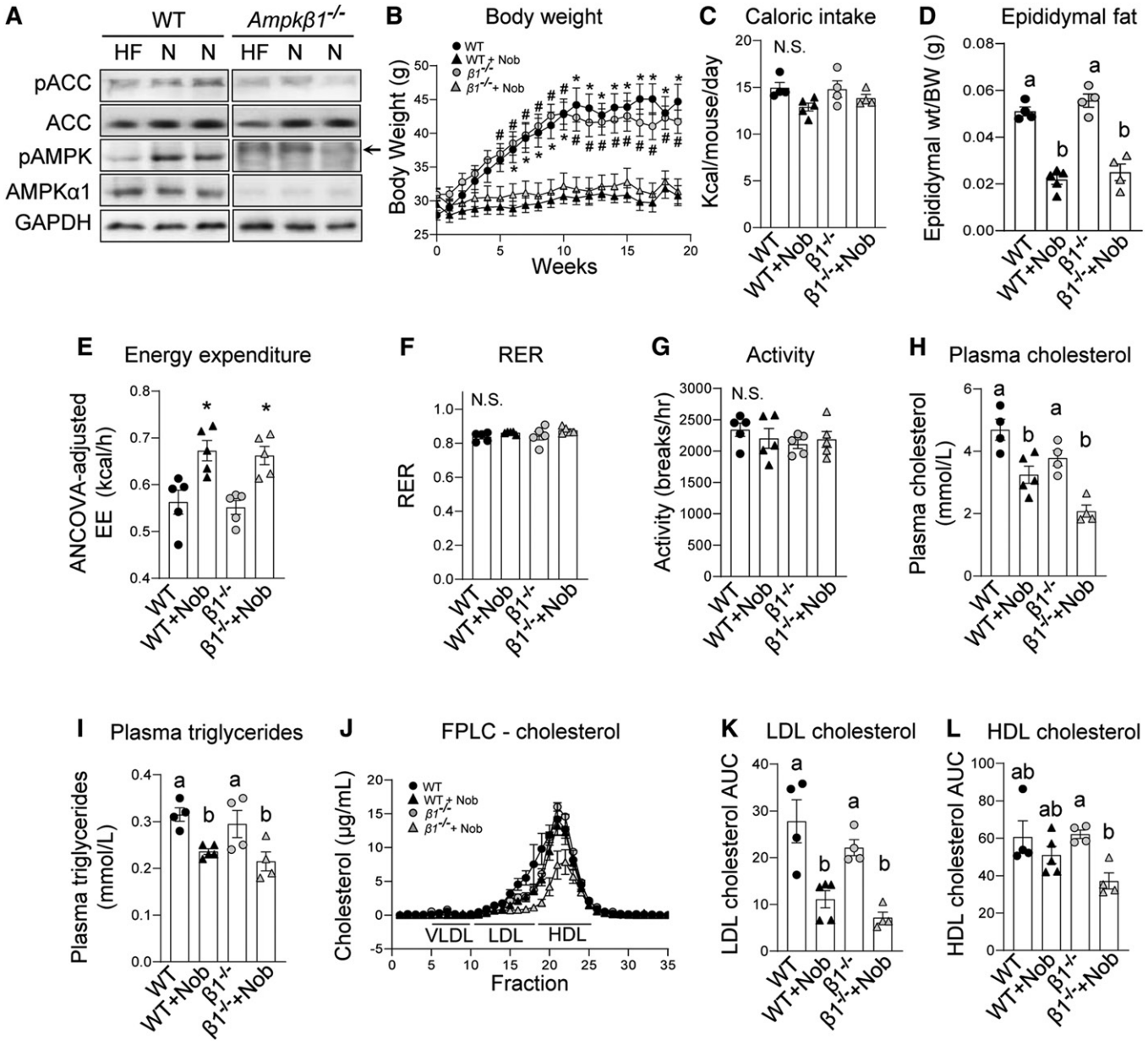

Fig. 2. Nobiletin attenuates body weight, adiposity, and plasma lipids and enhances energy expenditure in both HFHC diet-fed *Ampkβ1*$^{-/-}$ and WT mice. WT and *Ampkβ1*$^{-/-}$ mice were fed a HFHC diet (HF) alone or HFHC plus nobiletin (+Nob) for 18 weeks, n = 5–6 per group. A: Immunoblot of pAMPK, AMPK, pACC, and ACC in liver lysates from WT and *Ampkβ1*$^{-/-}$ mice fed a HFHC diet (HF) or a HFHC diet + nobiletin (N). Lysates were run on the same immunoblot. The slower running band (arrow) in the pAMPK blot in the *Ampkβ1*$^{-/-}$ liver sample is nonspecific. B: Body weight measured weekly. * or # indicates a statistical difference from nobiletin-treated mice within the same genotype, determined by two-way ANOVA with repeated measures analyses, $P < 0.05$. C: Mean daily caloric intake measured weekly. D: Adiposity assessed as epididymal fat pad weight/total body weight. E: ANCOVA-adjusted mean energy expenditure (kilocalories per hour) over 24 h. F: RER over 24 h. G: Mean ambulatory activity (breaks/hour) over 24 h. H: Plasma cholesterol concentrations. I: Plasma TG concentrations. J: Plasma cholesterol FPLC tracing. K: Plasma LDL-C AUC calculations. L: Plasma HDL-C AUC calculations. Data represent the mean ± SEM. Different letters indicate statistical differences by ANOVA with post hoc Tukey's test ($P < 0.05$). N.S., no significant difference.

Nobiletin supplementation increased hepatic FA oxidation in both genotypes (Fig. 3I).

Nobiletin attenuates hepatic steatosis and metabolic dysregulation in HFHC diet-fed *AccDKI* mice

AMPK phosphorylates and inhibits ACC thereby reducing malonyl-CoA, a critical substrate for de novo lipogenesis and inhibitor of FA oxidation (12, 13). As AMPKβ1 deletion only significantly reduces AMPK activity in hepatocytes (30) and macrophages (41), residual AMPK in other tissues may be important for mediating the beneficial effects of nobiletin in vivo. Therefore, to assess the importance of AMPK phosphorylation of ACC in the metabolic protection mediated by nobiletin, we utilized *AccDKI* mice harboring alanine knock-in mutations at the AMPK phosphorylation sites in both ACC1 and ACC2 (36), which effectively prevents the inhibitory phosphorylation of ACC by activated AMPK in all tissues. WT and *AccDKI* littermate mice were fed a

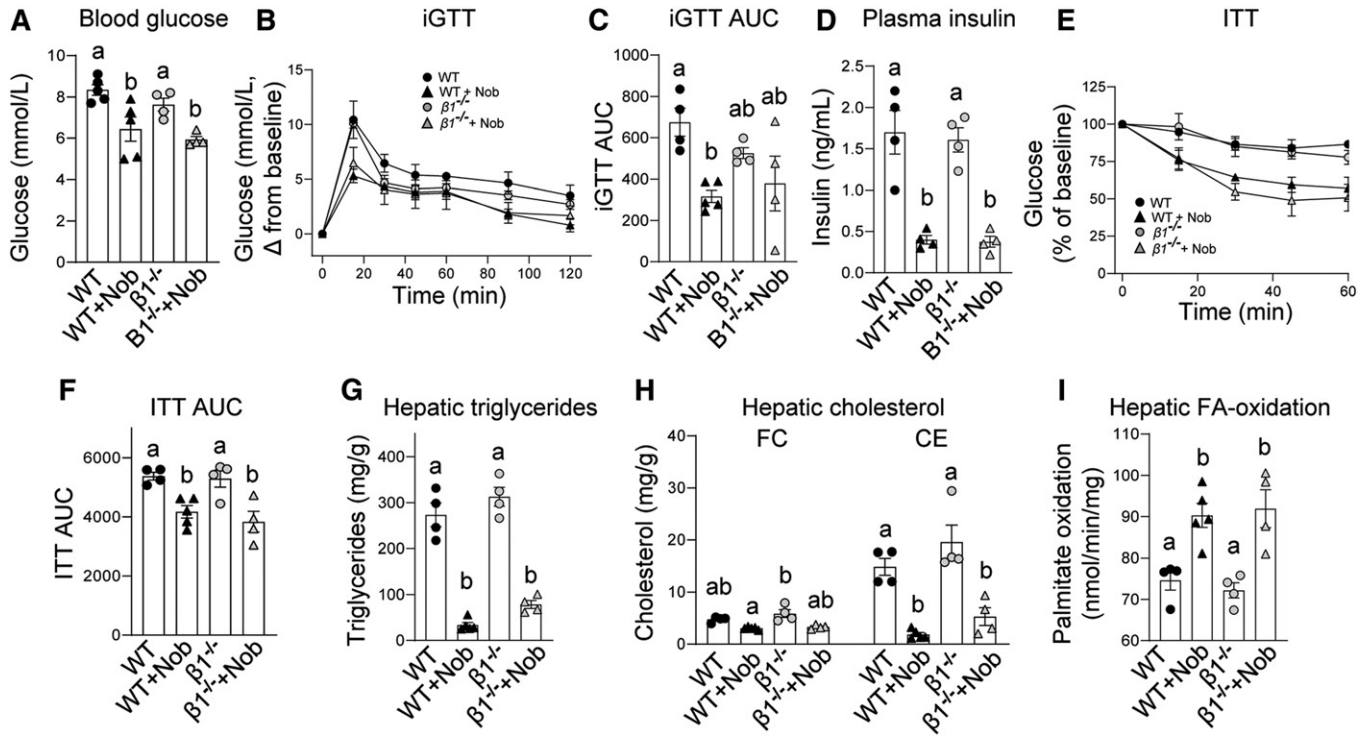

Fig. 3. Nobiletin improves glucose and insulin tolerance, decreases hepatic steatosis, and enhances hepatic FA oxidation in both HFHC diet-fed *Ampkβ1*$^{-/-}$ and WT mice. WT and *Ampkβ1*$^{-/-}$ mice were fed a HFHC diet (HF) alone or a HFHC diet plus nobiletin (+Nob) for 18 weeks, n = 5–6 per group. A: Blood glucose concentrations. B: iGTT. C: AUC for iGTT. D: Plasma insulin concentrations. E: ITT, as percent of baseline glucose. F: AUC for ITT, G: Hepatic TG concentrations. H: Hepatic FC and CE concentrations. I: Hepatic FA oxidation. Data represent the mean ± SEM. Different letters indicate statistical differences by ANOVA with post hoc Tukey's test ($P < 0.05$).

HFHC diet with or without nobiletin supplementation for 18 weeks. Consistent with previous studies (36), pACC was completely absent in the livers of *AccDKI* mice fed either HFHC diet or HFHC diet supplemented with nobiletin (**Fig. 4A**). pAMPK and AMPK were not consistently affected by genotype or diet. *AccDKI* mice gained the same amount of body weight in response to the HFHC diet as WT mice (Fig. 4B). Nobiletin prevented diet-induced weight gain in both *AccDKI* and WT mice. Caloric intake was unaffected by nobiletin treatment (Fig. 4C). eWAT depot weights were similar between *AccDKI* and WT mice and were markedly reduced with nobiletin supplementation (∼50%) in both genotypes (Fig. 4D).

Energy expenditure, RER, and activity levels were not different between HFHC diet-fed *AccDKI* and WT mice (Fig. 4E–G). Nobiletin induced an ∼20% increase in total ANCOVA-adjusted energy expenditure in WT and *AccDKI* mice (Fig. 4E). RER and activity levels were unaffected by genotype or nobiletin treatment (Fig. 4F, G). Plasma TC and TG were not different between HFHC diet-fed *AccDKI* and WT mice (Fig. 4H, I). Nobiletin supplementation significantly decreased plasma cholesterol (∼30%) and plasma TG levels (∼25%) in both genotypes. FPLC profiles of plasma lipoproteins indicated that the nobiletin-induced reductions in LDL-C (∼33%) were similar in *AccDKI* and WT mice (Fig. 4J, K). Nobiletin did not affect HDL-C in either genotype.

Fasting blood glucose and plasma insulin concentrations in *AccDKI* mice were not different from WT mice (**Fig. 5A**, D). Addition of nobiletin to the HFHC diet decreased fasting blood glucose (∼18%) and reduced plasma insulin (∼57%) in both *AccDKI* and WT mice. Furthermore, nobiletin treatment significantly improved glucose tolerance (∼60% in iGTT AUC; Fig. 5B, C) and improved insulin sensitivity (∼20% in ITT AUC) similarly in *AccDKI* and WT mice (Fig. 5E, F). The elevated hepatic lipids in HFHC diet-fed WT mice were not different between *AccDKI* and WT mice (Fig. 5G, H). Nobiletin markedly reduced hepatic TG (∼50%) and CE (∼45%) in both genotypes. Nobiletin supplementation increased hepatic FA oxidation by ∼1.35-fold in *AccDKI* mice and by ∼1.27-fold in WT mice (Fig. 5I).

Nobiletin prevents obesity and metabolic dysregulation in HFHC diet-fed AMPK *iβ1β2AKO* mice

Nobiletin increases energy expenditure, protecting mice from obesity and insulin resistance (7). BAT and beige adipose tissue are important regulators of energy expenditure (32). *Ampkβ1*$^{-/-}$ mice have modest reductions in AMPK activity in adipose tissue (30). However, studies in mice lacking both AMPKβ1 and -β2 subunits specifically in adipocytes have shown that AMPK is required for maintaining BAT and beige adipose tissue thermogenesis; effects which are independent of ACC phosphorylation but instead involve the regulation of mitochondrial function (32). Therefore, to specifically investigate the role of adipocyte AMPK in the ability of nobiletin to correct diet-induced obesity and metabolic dysfunction, mice with inducible deficiency in adipose tissue AMPKβ1 and -β2 (*iβ1β2AKO*) were fed a HFHC

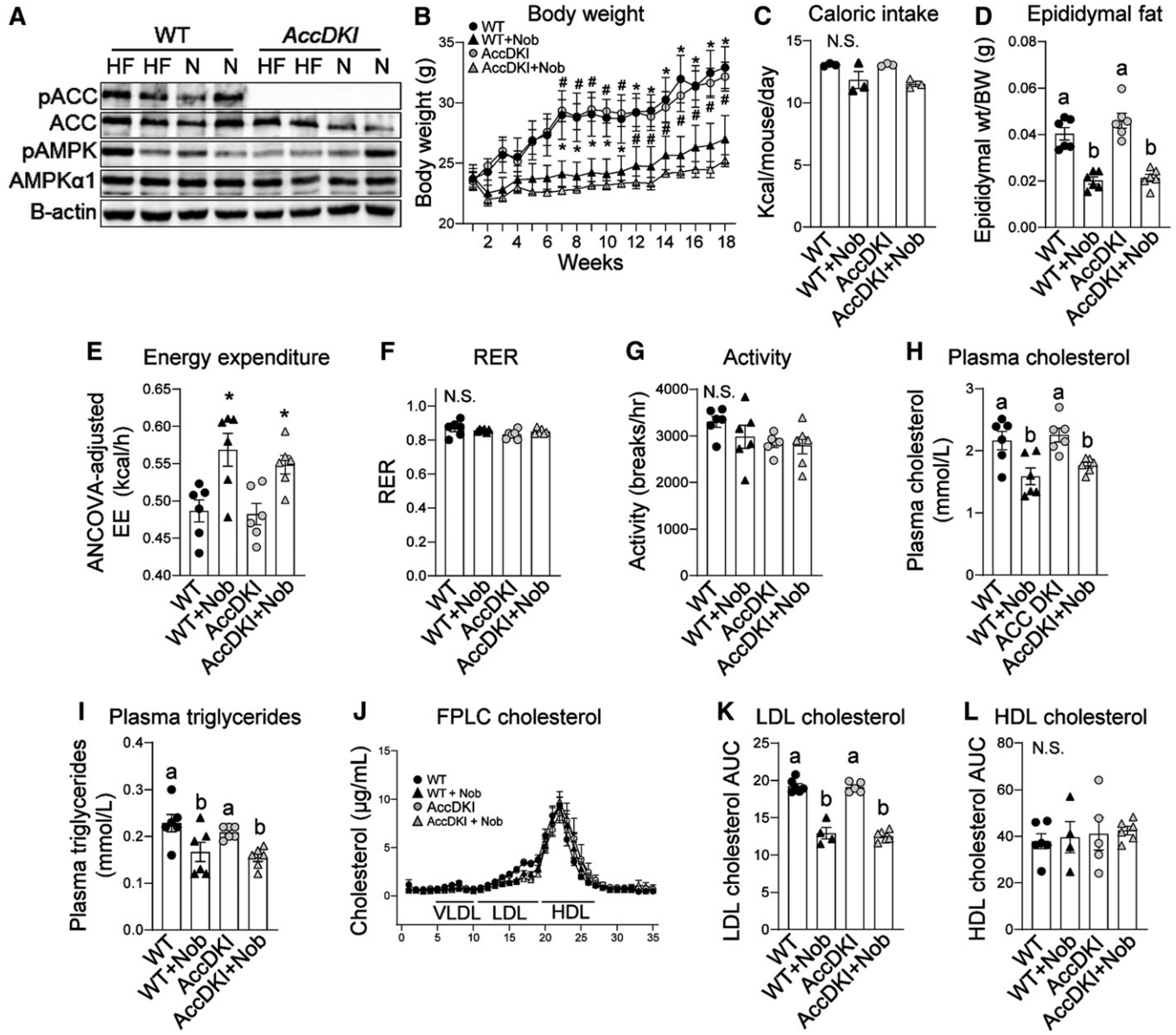

Fig. 4. Nobiletin attenuates body weight, adiposity, and plasma lipids and enhances energy expenditure in both HFHC diet-fed *AccDKI* and WT mice. WT and *AccDKI* mice were fed a HFHC diet (HF) alone or a HFHC diet plus nobiletin (+Nob) for 18 weeks, n = 6 per group. A: Immunoblot of pAMPK, AMPK, pACC, and ACC in liver lysates from WT and *AccDKI* mice fed a HFHC diet (HF) or a HFHC diet + nobiletin (N). Lysates were run on the same immunoblot. B: Body weight measured weekly. * or # indicates a statistical difference from nobiletin-treated mice within the same genotype, determined by two-way ANOVA with repeated measures analyses, $P < 0.05$. C: Mean caloric intake measured weekly. D: Adiposity assessed as epididymal fat pad weight/total body weight. E: ANCOVA adjusted mean energy expenditure (kilocalories per hour) over 24 h. F: RER over 24 h. G: Mean ambulatory activity (breaks/hour) over 24 h. H: Plasma cholesterol concentrations. I: Plasma TG concentrations. J: Plasma cholesterol FPLC tracing. K: Plasma LDL-C AUC calculations. L: Plasma HDL-C AUC calculations. Data represent the mean ± SEM. Different letters indicate statistical differences by ANOVA with post hoc Tukey's test ($P < 0.05$). N.S., no significant difference.

diet with or without nobiletin supplementation for 12 weeks. As expected, levels of AMPKβ1/β2 were reduced in the WAT of *iβ1β2AKO* mice, but most striking was the marked reduction of pACC in *iβ1β2AKO* mice fed either HFHC diet or HFHC diet plus nobiletin (**Fig. 6A**). The mRNA levels of *Ampkb1* and *Ampkb2* in eWAT were decreased ∼50% in *iβ1β2AKO* mice (Fig. 6B, C), consistent with previous findings demonstrating that residual AMPK activity in adipose tissue is from other cell types (e.g., resident stromal vascular cells) (32). Also consistent with previous studies (32), in response to the HFHC diet, *iβ1β2AKO* mice tended to gain slightly more weight compared with controls (Fig. 6D). Nobiletin prevented HFHC diet-induced weight gain to the same extent in both genotypes (Fig. 6D). Caloric intake was unaffected by nobiletin in both genotypes (Fig. 6E). eWAT and iWAT depot weights were similar in HFHC diet-fed *iβ1β2AKO* and control mice, and nobiletin supplementation reduced the weight of both depots to a similar degree (∼56%) in both genotypes (Fig. 6F, G). The histology of eWAT, iWAT, and BAT did not show any gross genotype

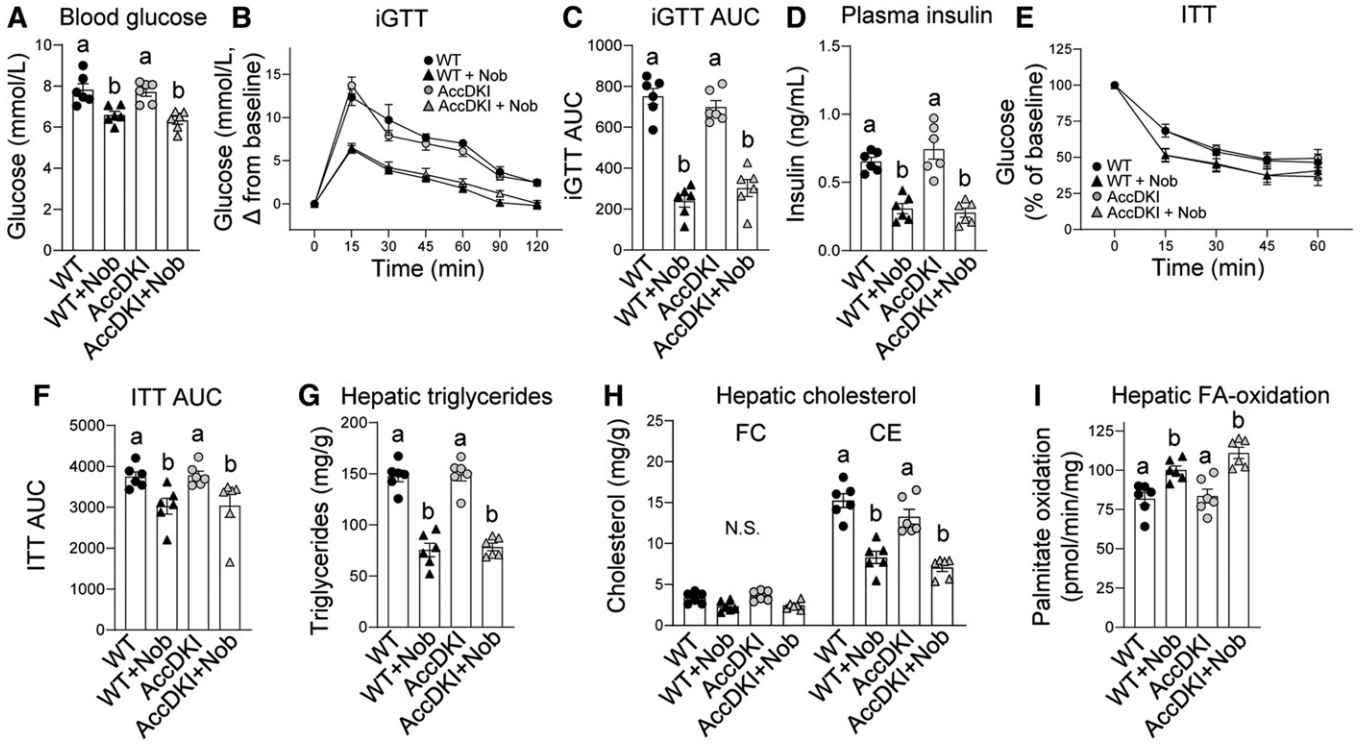

Fig. 5. Nobiletin improves glucose and insulin tolerance, decreases hepatic steatosis, and enhances hepatic FA oxidation in both HFHC diet-fed *AccDKI* and WT mice. WT and *AccDKI* mice were fed a HFHC diet (HF) alone or a HFHC diet plus nobiletin (+Nob) for 18 weeks, n = 6 per group. A: Blood glucose concentrations. B: iGTT. C: AUC for iGTT. D: Plasma insulin concentrations. E: ITT, as percent of baseline glucose. F: AUC for ITT. G: Hepatic TG concentrations. H: Hepatic FC and CE concentrations. I: Hepatic FA oxidation. Data represent the mean ± SEM. Different letters indicate statistical differences by ANOVA with post hoc Tukey's test ($P < 0.05$). N.S., no significant difference.

differences in HFHC diet-fed mice (Fig. 6H). Nobiletin treatment resulted in smaller adipocytes in eWAT and iWAT and smaller lipid droplets in BAT of both *iβ1β2AKO* and control mice (Fig. 6H). Quantitation of adipocyte area distribution, mean adipocyte area, and adipocyte number in eWAT revealed no difference between HFHC diet-fed *iβ1β2AKO* mice and controls (Fig. 6I–K). Nobiletin improved adipocyte area distribution and decreased mean adipocyte area and number to similar levels in both genotypes. Similar patterns were observed for nobiletin-induced reductions in iWAT adipocyte size and number in both *iβ1β2AKO* mice and controls (supplemental Fig. S2A–C). As adipose tissue browning of iWAT has been shown to be important for weight loss in some studies and may be modulated by nobiletin (42), we measured the expression of *Ucp1* and other known regulators of adipose tissue browning. Despite the same nobiletin-induced decreases in iWAT mass (Fig. 6F), nobiletin treatment increased the mRNA of *Ucp1* and *Tbx1* in control iWAT but not in *iβ1β2AKO* iWAT. Furthermore, nobiletin increased *Cd137* mRNA in *iβ1β2AKO* iWAT but not in control iWAT (Fig. 6L–O). This inconsistency in expression of browning markers between genotypes together with the marked reduction by nobiletin of adipose tissue depots in both genotypes suggests that the effect of nobiletin did not involve browning of WAT.

Parameters for total ANCOVA-adjusted energy expenditure, RER, and activity levels were not different between HFHC diet-fed *iβ1β2AKO* and control mice (**Fig. 7A–**C). Nobiletin induced a similar increase in energy expenditure (∼30%) in both *iβ1β2AKO* and control mice (Fig. 7A). RER and activity levels were unaffected by genotype or nobiletin treatment (Fig. 7B, C). Plasma concentrations of total TG and cholesterol in HFHC diet-fed *iβ1β2AKO* mice were not different from controls (Fig. 7D, E). Nobiletin supplementation significantly decreased plasma TG and cholesterol to similar extents in each genotype (Fig. 7D, E). FPLC profiles of plasma lipoproteins indicated that the nobiletin-induced reductions in LDL-C (∼65%) and HDL-C (∼50%) were similar for *iβ1β2AKO* and control mice (Fig. 7F–H).

Consistent with previous studies (32), fasting blood glucose, glucose intolerance, plasma insulin, and insulin intolerance were elevated in HFHC diet-fed *iβ1β2AKO* mice compared with controls; although in the present study, these genotype differences were not statistically significant (Fig. 7I–N). Addition of nobiletin to the HFHC diet decreased fasting blood glucose (∼36%) and improved glucose tolerance (∼46%) similarly in both genotypes (Fig. 7I–K). Nobiletin decreased plasma insulin (∼90%) and improved insulin tolerance (∼27%) in *iβ1β2AKO* mice to the same extent as in control mice (Fig. 7L–N). Diet-induced hepatic steatosis was similar in *iβ1β2AKO* mice and control mice (Fig. 7O, P). Nobiletin significantly decreased TG (∼86%), FC (∼25%), and CE (∼80%) such that the marked reduction of each lipid was similar in both genotypes.

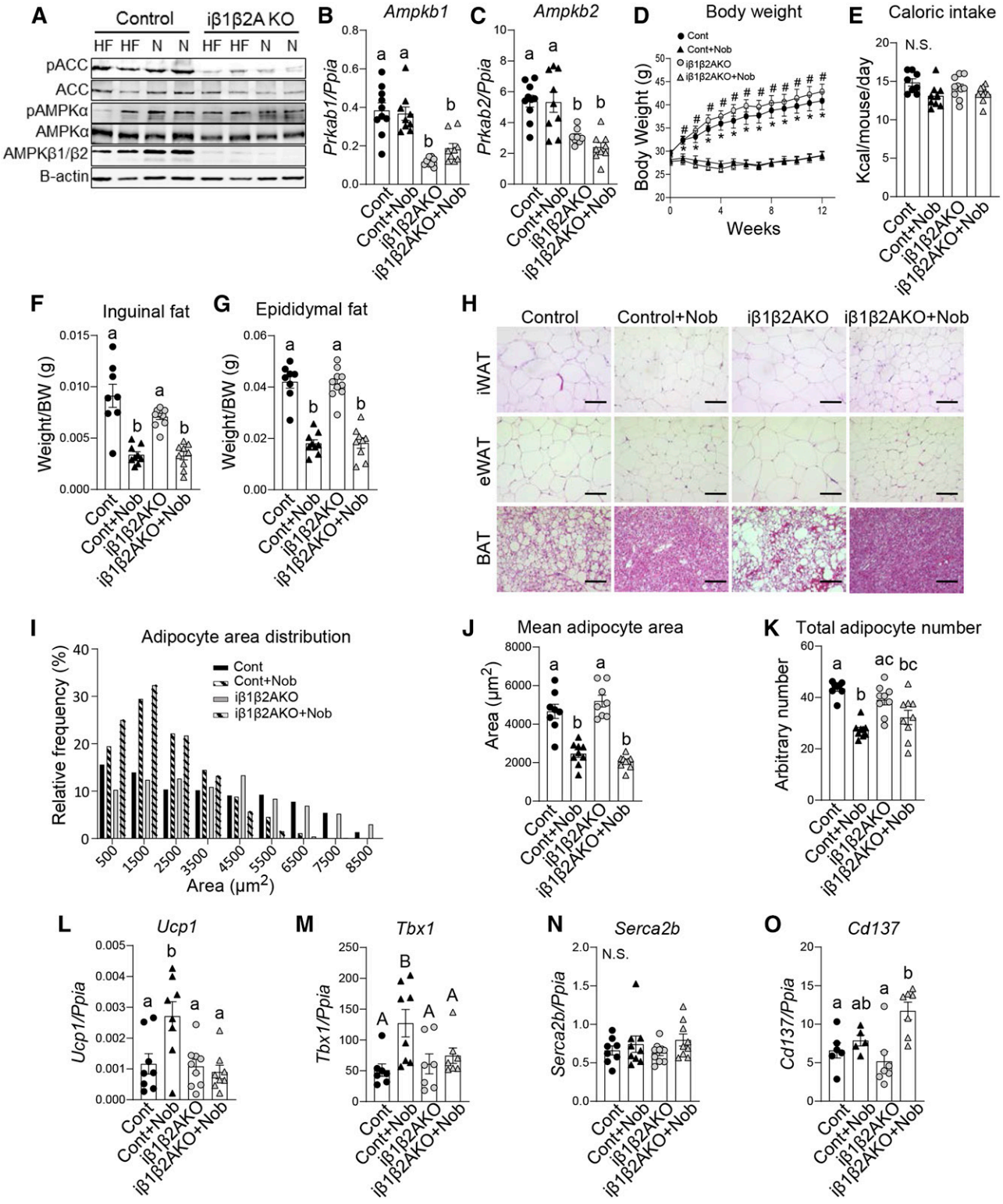

Fig. 6. Nobiletin attenuates body weight and adiposity and normalizes adipocyte morphology in both HFHC diet-fed *iβ1β2AKO* and WT mice. WT and *iβ1β2AKO* mice were fed a HFHC diet (HF) alone or a HFHC diet plus nobiletin (+Nob) for 12 weeks, n = 8–9 per group. A: Immunoblot of pAMPK, AMPK, pACC, and ACC in liver lysates from WT and *iβ1β2AKO* mice fed a HFHC diet (HF) or a HFHC diet + nobiletin (N). Lysates were run on the same immunoblot. B: Adipose tissue (iWAT) *Ampkb1* mRNA. C: Adipose tissue (iWAT) *Ampkb2* mRNA. D: Body weight measured weekly. * or # indicates a statistical difference from nobiletin-treated mice within the same genotype, determined by two-way ANOVA with repeated measures analyses, $P < 0.05$. E: Mean daily caloric intake measured weekly. F: Adiposity assessed as inguinal fat pad weight/total body weight. G: Adiposity assessed as epididymal fat pad weight/total body weight. H: Representative images of iWAT, eWAT, and BAT stained with H&E. Scale bar is 100 μm. I: Frequency distribution of adipocyte area in eWAT. J: Mean adipocyte area in eWAT. K: Total adipocyte number in eWAT calculated as the mean number of cells per field of view X weight of eWAT. L–O: Adipose tissue (iWAT) *Ucp1*, *Tbx1*, *Serca2b*, and *Cd137* mRNA. Data represent the mean ± SEM. Different letters indicate statistical differences by ANOVA with post hoc Tukey's test ($P < 0.05$). N.S.; no significant difference.

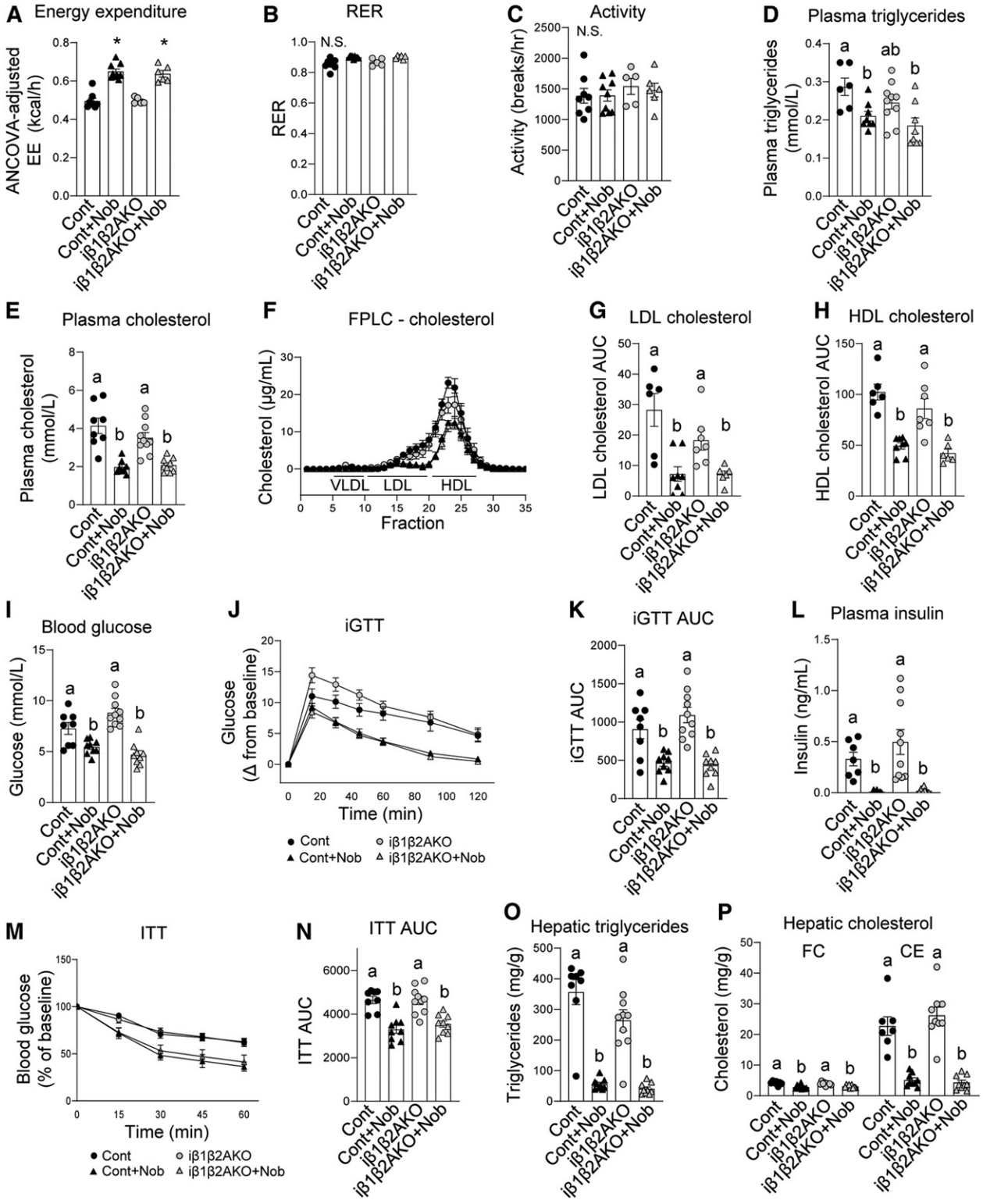

Fig. 7. Nobiletin decreases plasma lipids, enhances energy expenditure, improves glucose and insulin tolerance, and decreases hepatic steatosis in both HFHCdiet-fed *iβ1β2AKO* and WT mice. WT and *iβ1β2AKO* mice were fed a HFHC diet (HF) alone or a HFHC diet plus nobiletin (+Nob) for 12 weeks, n = 8–9 per group. A: ANCOVA adjusted mean energy expenditure (kilocalories per hour) over 24 h. B: RER over 24 h. C: Mean ambulatory activity (breaks per hour) over 24 h. D: Plasma TG concentrations. E: Plasma cholesterol concentrations. F: Plasma cholesterol FPLC tracing. G: Plasma LDL-C AUC calculations. H: Plasma HDL-C AUC calculations. I: Blood glucose concentrations. J: iGTT. K: AUC for iGTT. L: Plasma insulin concentrations. M: ITT, as percent of baseline glucose. N: AUC for ITT. O: Hepatic TG concentrations. P: Hepatic FC and CE concentrations. Data represent the mean ± SEM. Different letters indicate statistical differences by ANOVA with post hoc Tukey's test ($P < 0.05$). N.S., no significant difference.

DISCUSSION

The specific mechanisms by which nobiletin mediates metabolic protection in high-fat-fed mice have not been established. The central role of AMPK as an energy sensor together with studies in cultured cells suggested that AMPK is a primary target of nobiletin. In the present studies, nobiletin induced a moderate increase in phosphorylation of AMPK and its downstream target ACC in primary mouse hepatocytes, which was associated with suppressed FA synthesis and increased FA oxidation. As expected, nobiletin-induced ACC phosphorylation was lost in *Ampkβ1*$^{-/-}$ hepatocytes. However, nobiletin continued to suppress FA synthesis and enhance FA oxidation in hepatocytes from both *Ampkβ1*$^{-/-}$ and WT mice. In mice fed a HFHC diet, nobiletin supplementation robustly prevented obesity, hepatic lipid accumulation, dyslipidemia, insulin resistance, and improved energy expenditure in *Ampkβ1*$^{-/-}$, *AccDKI*, and *iβ1β2AKO* mice to the same extent as their respective WT controls. These studies demonstrate that metabolic protection by nobiletin in vivo is conferred independently of hepatic or adipocyte AMPK.

Nobiletin treatment of primary mouse hepatocytes increased the phosphorylation of AMPK and ACC, which was associated with reduced FA synthesis and increased FA oxidation. However, in nobiletin-treated *Ampkβ1*$^{-/-}$ hepatocytes, which were incapable of AMPK and ACC phosphorylation, the suppression of FA synthesis and enhancement of FA oxidation were maintained, indicating that the ability of nobiletin to regulate FA metabolism did not require AMPK. While previous studies in primary mouse hepatocytes (21) and HepG2 cells (22) have suggested a role for AMPK in the mechanism of action of nobiletin, cells deficient in AMPK or ACC phosphorylation were not used to establish the dependency of nobiletin-induced regulation of cellular lipid metabolism on AMPK. It is not entirely clear why nobiletin increased the phosphorylation of AMPK and ACC in cultured hepatocytes but not in vivo in mouse liver. It is possible that the modest activation of AMPK in hepatocytes by nobiletin is unique to cell culture. It is likely that active metabolites of nobiletin generated by the gut microbiota (43) or by hepatic CYP450 conversion of the parent compound (44) contribute significantly to the metabolic protection observed in mice, whereas nobiletin itself is the primary metabolic effector in cultured hepatocytes [(7) and Fig. 1]. It is possible that nobiletin activates AMPK in cultured hepatocytes, whereas active nobiletin metabolites generated in vivo do not. Contrary to this idea, our acute studies in mice (supplemental Fig. S1) revealed that intraperitoneal administration of nobiletin (bypasses the gut) followed by analyses of liver samples obtained 90 min postinjection (prior to significant hepatic metabolism of nobiletin) did not induce phosphorylation of AMPK and ACC. Nevertheless, nobiletin-induced AMPK phosphorylation in cultured hepatocytes is not responsible for nobiletin's ability to regulate cellular FA synthesis or oxidation. These results underscore the importance of examining hepatocytes deficient in AMPK for defining the functional role of AMPK in the mechanism of action of metabolic regulators.

It was anticipated that in *Ampkβ1*$^{-/-}$ mice with hepatic deficiency of AMPK, the metabolic protection by nobiletin would be attenuated; however, this was not the case. Addition of nobiletin to the HFHC diet attenuated adiposity, hepatic steatosis, and hyperlipidemia, and improved energy expenditure and glucose homeostasis as effectively in *Ampkβ1*$^{-/-}$ mice as in WT mice, indicating that nobiletin-induced prevention of metabolic dysregulation was independent of hepatic AMPK. These results have parallels to the effects of the ATP citrate lyase inhibitor, bempedoic acid, which activates AMPK in cultured hepatocytes and in the livers of high-fat fed *Apoe*$^{-/-}$ mice (45). However, bempedoic acid lowered liver lipids, hepatocyte lipogenesis, LDL-C, and aortic cholesterol to the same extent in *Apoe*$^{-/-}$*;Ampkβ1*$^{-/-}$ double knockout mice as it did in *Apoe*$^{-/-}$ mice (45). In addition, although salicylate at high concentrations activates hepatic AMPK in WT mice, clinically relevant concentrations of salicylate (2.5 g/kg of diet) decreased adiposity and liver lipid content and improved glucose homeostasis just as effectively in *Ampkβ1*$^{-/-}$ mice as in WT mice (46). Rather, the salicylate-induced metabolic effects were shown to be due to the ability of salicylate to stimulate mitochondrial conductance resulting in mitochondrial uncoupling. It is possible that nobiletin also acts as a metabolic uncoupler, although this has not been examined. Previous studies demonstrating an increase in hepatic mitochondrial DNA in nobiletin-treated high-fat diet-fed mice is consistent with this idea (7).

In *Ampkβ1*$^{-/-}$ mice, approximately 10% of hepatic AMPK activity is retained (30), which may be sufficient to mediate some downstream phosphorylation. Furthermore, it is possible that aspects of nobiletin-mediated regulation of lipid metabolism involve ACC phosphorylation independent of AMPK. Nevertheless, nobiletin was equally effective in preventing metabolic dysregulation in HFHC diet-fed *AccDKI* mice and in WT mice, clearly demonstrating that the protective effects of nobiletin were independent of inhibitory phosphorylation of ACC. These results differ from the effects of metformin. In contrast to nobiletin, high-fat diet-fed *AccDKI* mice were refractory to the lipid-lowering and insulin-sensitizing effects of metformin, and metformin had no effect on body weight or adiposity in either genotype (36). These findings imply that the mechanisms underlying nobiletin-induced metabolic protection differ from those of metformin.

Obesity is associated with reduced AMPK activity in adipose tissue, and dysfunctional BAT contributes to diet-induced obesity and insulin resistance (47–49). Recent studies reported that adult *iβ1β2AKO* mice had impairments in cold tolerance and were resistant to β-adrenergic activation of BAT and browning of WAT due to impaired mitochondrial structure and function (32). In addition, hepatic steatosis and glucose and insulin intolerance were amplified in high-fat-fed *iβ1β2AKO* mice (32). Therefore, we investigated the impact of nobiletin in HFHC diet-fed *iβ1β2AKO* mice. Reductions in iWAT and eWAT mass and adipocyte number and area, and the improvement in

adipocyte morphology in nobiletin-treated *iβ1β2AKO* mice were the same as in control mice. Furthermore, nobiletin supplementation attenuated hepatic steatosis, dyslipidemia, and insulin resistance, and improved energy expenditure to a similar extent in both genotypes, indicating that prevention of metabolic dysregulation by nobiletin does not require adipocyte AMPK. The only differences between genotypes in response to nobiletin were the increases in the browning markers *Ucp1* and *Tbx1* mRNA in control iWAT but not in *iβ1β2AKO* iWAT, and the increase in *Cd137* mRNA in nobiletin-treated *iβ1β2AKO* iWAT but not control iWAT. Previous studies in chow-fed *iβ1β2AKO* mice demonstrated that chronic β-adrenergic receptor agonist treatment did not lower iWAT mass but increased the number of multilocular beige adipocytes and increased *Ucp1* expression in the iWAT of control mice, but not in *iβ1β2AKO* mice (32). Consistent with these results, nobiletin increased *Ucp1* expression only in control mice; however, nobiletin decreased iWAT mass equally and multilocular beige adipocytes were not observed in either nobiletin-treated genotype. Taken together with the similar improvements in other adipocyte parameters in both genotypes, these findings suggest that adipocyte browning was not involved in nobiletin's ability to attenuate adiposity. In addition, these results imply that the beneficial effects of nobiletin on adipose tissue mass and other metabolic parameters do not involve β-adrenergic activation of BAT or WAT.

The mechanism(s) through which nobiletin regulates lipid metabolism, adiposity, and insulin sensitivity are not fully understood. In mice, nobiletin suppressed hepatic FA synthesis and upregulated hepatic FA oxidation, independent of peroxisomal proliferation (7); however, the upstream effectors governing these effects have remained elusive. Experiments in cultured hepatocytes and murine liver indicated that nobiletin does not activate PPARα, PPARγ, or PPARβ/δ (7). The effects of nobiletin are not mediated by leptin or Fgf21, as evidenced by metabolic protection in *Ob/Ob* mice (50) or in high-fat diet-fed *Fgf21*$^{-/-}$ mice [(4) and unpublished observations]. The ability of nobiletin to prevent metabolic dysregulation has been associated with the direct activation of the retinoic acid receptor-related orphan receptor (ROR), resulting in enhanced amplitude of circadian rhythms in obese mice (51). However, the specific metabolic pathways affected have not been identified. Recent studies in mouse skeletal muscle revealed that nobiletin activation of ROR-dependent gene expression stimulated mitochondrial respiratory complex function and suppressed formation of reactive oxygen species (52), consistent with our previous in vivo studies linking nobiletin to mitochondrial expansion in liver (7). In HepG2 cells, Qi et al. (21) reported that nobiletin amplified glucose uptake and suppressed palmitate-induced lipogenesis, which required activation of AMPK in a clock gene (*Bmal1*)-dependent manner. The present study clearly demonstrates that any ROR-dependent metabolic effects of nobiletin in vivo do not require AMPK activation in the liver or adipose tissue.

Metabolites of nobiletin derived from gut microbes have been identified and shown to accumulate in mouse colonic mucosa at concentrations exceeding that of nobiletin by ∼20-fold (43). These demethylated nobiletin metabolites have been shown to have stronger anti-cancer effects than the parent compound in human colon cancer cells (43), raising the possibility that metabolic protection by nobiletin in vivo is primarily conferred by these metabolites. Furthermore, these metabolites have been shown to inhibit the induction of iNOS, the inflammatory response, and scavenger receptor expression in LPS-treated macrophage cell lines (53–55), properties that may be related to cardiovascular protection. However, the molecular targets and cardiometabolic effects of these metabolites in vivo have not been reported. Thus, the extent to which microbiota-derived nobiletin metabolites contribute to the prevention of metabolic dysregulation and atherosclerosis in mice warrants further investigation.

In summary, the mechanism underlying the ability of nobiletin to achieve metabolic protection in mice is independent of AMPK activation, thereby bypassing the central regulator of cellular energy homeostasis. In primary mouse hepatocytes, nobiletin suppressed FA synthesis and enhanced FA oxidation to the same extent in both *Ampkβ1*$^{-/-}$ and WT cells. Compared with WT or control mice, nobiletin was equally effective in preventing metabolic dysregulation in three models of HFHC diet-fed mice: mice deficient in hepatic AMPK, mice incapable of inhibitory phosphorylation of ACC, and mice with adipocyte-specific deficiency of AMPK. These studies highlight the potential therapeutic utility of the citrus flavonoid nobiletin, especially in the context of metabolic syndrome, and the need for further studies to investigate primary mechanisms of action.

The authors would like to thank Jane Edwards (Robarts Research Institute) for assistance with quantitative RT-PCR and Robert Gros (Robarts Research Institute) for the use of metabolic cages.

REFERENCES

1. Al Rifai, M., M. G. Silverman, K. Nasir, M. J. Budoff, R. Blankstein, M. Szklo, R. Katz, R. S. Blumenthal, and M. J. Blaha. 2015. The association of nonalcoholic fatty liver disease, obesity, and metabolic syndrome, with systemic inflammation and subclinical atherosclerosis: the Multi-Ethnic Study of Atherosclerosis (MESA). *Atherosclerosis.* **239:** 629–633.
2. Nolan, P. B., G. Carrick-Ranson, J. W. Stinear, S. A. Reading, and L. C. Dalleck. 2017. Prevalence of metabolic syndrome and metabolic syndrome components in young adults: a pooled analysis. *Prev. Med. Rep.* **7:** 211–215.
3. Mulvihill, E. E., A. C. Burke, and M. W. Huff. 2016. Citrus flavonoids as regulators of lipoprotein metabolism and atherosclerosis. *Annu. Rev. Nutr.* **36:** 275–299.
4. Assini, J. M., E. E. Mulvihill, A. C. Burke, B. G. Sutherland, D. E. Telford, S. S. Chhoker, C. G. Sawyez, M. Drangova, A. C. Adams, A. Kharitonenkov, et al. 2015. Naringenin prevents obesity, hepatic steatosis, and glucose intolerance in male mice independent of fibroblast growth factor 21. *Endocrinology.* **156:** 2087–2102.
5. Assini, J. M., E. E. Mulvihill, B. G. Sutherland, D. E. Telford, C. G. Sawyez, S. L. Felder, S. Chhoker, J. Y. Edwards, R. Gros, and M. W. Huff. 2013. Naringenin prevents cholesterol-induced systemic inflammation, metabolic dysregulation, and atherosclerosis in *Ldlr*$^{-/-}$ mice. *J. Lipid Res.* **54:** 711–724.
6. Mulvihill, E. E., E. M. Allister, B. G. Sutherland, D. E. Telford, C. G. Sawyez, J. Y. Edwards, J. M. Markle, R. A. Hegele, and M. W. Huff. 2009. Naringenin prevents dyslipidemia, apolipoprotein B

overproduction, and hyperinsulinemia in LDL receptor-null mice with diet-induced insulin resistance. *Diabetes.* **58:** 2198–2210.
7. Mulvihill, E. E., J. M. Assini, J. K. Lee, E. M. Allister, B. G. Sutherland, J. B. Koppes, C. G. Sawyez, J. Y. Edwards, D. E. Telford, A. Charbonneau, et al. 2011. Nobiletin attenuates VLDL overproduction, dyslipidemia, and atherosclerosis in mice with diet-induced insulin resistance. *Diabetes.* **60:** 1446–1457.
8. Mulvihill, E. E., J. M. Assini, B. G. Sutherland, A. S. DiMattia, M. Khami, J. B. Koppes, C. G. Sawyez, S. C. Whitman, and M. W. Huff. 2010. Naringenin decreases progression of atherosclerosis by improving dyslipidemia in high-fat-fed low-density lipoprotein receptor-null mice. *Arterioscler. Thromb. Vasc. Biol.* **30:** 742–748.
9. Li, R. W., A. G. Theriault, K. Au, T. D. Douglas, A. Casaschi, E. M. Kurowska, and R. Mukherjee. 2006. Citrus polymethoxylated flavones improve lipid and glucose homeostasis and modulate adipocytokines in fructose-induced insulin resistant hamsters. *Life Sci.* **79:** 365–373.
10. Burke, A. C., B. G. Sutherland, D. E. Telford, M. R. Morrow, C. G. Sawyez, J. Y. Edwards, M. Drangova, and M. W. Huff. 2018. Intervention with citrus flavonoids reverses obesity and improves metabolic syndrome and atherosclerosis in obese $Ldlr^{-/-}$ mice. *J. Lipid Res.* **59:** 1714–1728.
11. Zhang, N., Z. Yang, S. Z. Xiang, Y. G. Jin, W. Y. Wei, Z. Y. Bian, W. Deng, and Q. Z. Tang. 2016. Nobiletin attenuates cardiac dysfunction, oxidative stress, and inflammatory in streptozotocin: induced diabetic cardiomyopathy. *Mol. Cell. Biochem.* **417:** 87–96.
12. Steinberg, G. R., and B. E. Kemp. 2009. AMPK in health and disease. *Physiol. Rev.* **89:** 1025–1078.
13. Steinberg, G. R., and D. Carling. 2019. AMP-activated protein kinase: the current landscape for drug development. *Nat. Rev. Drug Discov.* **18:** 527–551.
14. Fullerton, M. D. 2016. AMP-activated protein kinase and its multifaceted regulation of hepatic metabolism. *Curr. Opin. Lipidol.* **27:** 172–180.
15. O'Neill, H. M., G. P. Holloway, and G. R. Steinberg. 2013. AMPK regulation of fatty acid metabolism and mitochondrial biogenesis: implications for obesity. *Mol. Cell. Endocrinol.* **366:** 135–151.
16. Li, Y., S. Xu, M. M. Mihaylova, B. Zheng, X. Hou, B. Jiang, O. Park, Z. Luo, E. Lefai, J. Y. Shyy, et al. 2011. AMPK phosphorylates and inhibits SREBP activity to attenuate hepatic steatosis and atherosclerosis in diet-induced insulin-resistant mice. *Cell Metab.* **13:** 376–388.
17. Hawley, S. A., F. A. Ross, C. Chevtzoff, K. A. Green, A. Evans, S. Fogarty, M. C. Towler, L. J. Brown, O. A. Ogunbayo, A. M. Evans, et al. 2010. Use of cells expressing gamma subunit variants to identify diverse mechanisms of AMPK activation. *Cell Metab.* **11:** 554–565.
18. Cool, B., B. Zinker, W. Chiou, L. Kifle, N. Cao, M. Perham, R. Dickinson, A. Adler, G. Gagne, R. Iyengar, et al. 2006. Identification and characterization of a small molecule AMPK activator that treats key components of type 2 diabetes and the metabolic syndrome. *Cell Metab.* **3:** 403–416.
19. Zhou, G., R. Myers, Y. Li, Y. Chen, X. Shen, J. Fenyk-Melody, M. Wu, J. Ventre, T. Doebber, N. Fujii, et al. 2001. Role of AMP-activated protein kinase in mechanism of metformin action. *J. Clin. Invest.* **108:** 1167–1174.
20. Zang, M., S. Xu, K. A. Maitland-Toolan, A. Zuccollo, X. Hou, B. Jiang, M. Wierzbicki, T. J. Verbeuren, and R. A. Cohen. 2006. Polyphenols stimulate AMP-activated protein kinase, lower lipids, and inhibit accelerated atherosclerosis in diabetic LDL receptor-deficient mice. *Diabetes.* **55:** 2180–2191.
21. Qi, G., R. Guo, H. Tian, L. Li, H. Liu, Y. Mi, and X. Liu. 2018. Nobiletin protects against insulin resistance and disorders of lipid metabolism by reprogramming of circadian clock in hepatocytes. *Biochim. Biophys. Acta Mol. Cell Biol. Lipids.* **1863:** 549–562.
22. Yuk, T., Y. Kim, J. Yang, J. Sung, H. S. Jeong, and J. Lee. 2018. Nobiletin inhibits hepatic lipogenesis via activation of AMP-activated protein kinase. *Evid. Based Complement. Alternat. Med.* **2018:** 7420265.
23. Bojic, L. A., D. E. Telford, M. D. Fullerton, R. J. Ford, B. G. Sutherland, J. Y. Edwards, C. G. Sawyez, R. Gros, B. E. Kemp, G. R. Steinberg, et al. 2014. PPARdelta activation attenuates hepatic steatosis in $Ldlr^{-/-}$ mice by enhanced fat oxidation, reduced lipogenesis, and improved insulin sensitivity. *J. Lipid Res.* **55:** 1254–1266.
24. Ford, R. J., M. D. Fullerton, S. L. Pinkosky, E. A. Day, J. W. Scott, J. S. Oakhill, A. L. Bujak, B. K. Smith, J. D. Crane, R. M. Blumer, et al. 2015. Metformin and salicylate synergistically activate liver AMPK, inhibit lipogenesis and improve insulin sensitivity. *Biochem. J.* **468:** 125–132.
25. Park, S. J., F. Ahmad, A. Philp, K. Baar, T. Williams, H. Luo, H. Ke, H. Rehmann, R. Taussig, A. L. Brown, et al. 2012. Resveratrol ameliorates aging-related metabolic phenotypes by inhibiting cAMP phosphodiesterases. *Cell.* **148:** 421–433.
26. Daval, M., F. Diot-Dupuy, R. Bazin, I. Hainault, B. Viollet, S. Vaulont, E. Hajduch, P. Ferre, and F. Foufelle. 2005. Anti-lipolytic action of AMP-activated protein kinase in rodent adipocytes. *J. Biol. Chem.* **280:** 25250–25257.
27. Vila-Bedmar, R., M. Lorenzo, and S. Fernandez-Veledo. 2010. Adenosine 5′-monophosphate-activated protein kinase-mammalian target of rapamycin cross talk regulates brown adipocyte differentiation. *Endocrinology.* **151:** 980–992.
28. Yin, W., J. Mu, and M. J. Birnbaum. 2003. Role of AMP-activated protein kinase in cyclic AMP-dependent lipolysis In 3T3-L1 adipocytes. *J. Biol. Chem.* **278:** 43074–43080.
29. Bauwens, J. D., E. G. Schmuck, C. R. Lindholm, R. L. Ertel, J. D. Mulligan, I. Hovis, B. Viollet, and K. W. Saupe. 2011. Cold tolerance, cold-induced hyperphagia, and nonshivering thermogenesis are normal in alpha(1)-AMPK-/- mice. *Am. J. Physiol. Regul. Integr. Comp. Physiol.* **301:** R473–R483.
30. Dzamko, N., B. J. van Denderen, A. L. Hevener, S. B. Jorgensen, J. Honeyman, S. Galic, Z. P. Chen, M. J. Watt, D. J. Campbell, G. R. Steinberg, et al. 2010. AMPK beta1 deletion reduces appetite, preventing obesity and hepatic insulin resistance. *J. Biol. Chem.* **285:** 115–122.
31. Wan, Z., J. Root-McCaig, L. Castellani, B. E. Kemp, G. R. Steinberg, and D. C. Wright. 2014. Evidence for the role of AMPK in regulating PGC-1 alpha expression and mitochondrial proteins in mouse epididymal adipose tissue. *Obesity (Silver Spring).* **22:** 730–738.
32. Mottillo, E. P., E. M. Desjardins, J. D. Crane, B. K. Smith, A. E. Green, S. Ducommun, T. I. Henriksen, I. A. Rebalka, A. Razi, K. Sakamoto, et al. 2016. Lack of adipocyte AMPK exacerbates insulin resistance and hepatic steatosis through brown and beige adipose tissue function. *Cell Metab.* **24:** 118–129.
33. Lone, J., H. A. Parray, and J. W. Yun. 2018. Nobiletin induces brown adipocyte-like phenotype and ameliorates stress in 3T3-L1 adipocytes. *Biochimie.* **146:** 97–104.
34. Tung, Y. C., S. Li, Q. Huang, W. L. Hung, C. T. Ho, G. J. Wei, and M. H. Pan. 2016. 5-Demethylnobiletin and 5-acetoxy-6,7,8,3′,4′-pentamethoxyflavone suppress lipid accumulation by activating the LKB1-AMPK pathway in 3T3-L1 preadipocytes and high fat diet-fed C57BL/6 mice. *J. Agric. Food Chem.* **64:** 3196–3205.
35. Choi, Y., Y. Kim, H. Ham, Y. Park, H. S. Jeong, and J. Lee. 2011. Nobiletin suppresses adipogenesis by regulating the expression of adipogenic transcription factors and the activation of AMP-activated protein kinase (AMPK). *J. Agric. Food Chem.* **59:** 12843–12849.
36. Fullerton, M. D., S. Galic, K. Marcinko, S. Sikkema, T. Pulinilkunnil, Z. P. Chen, H. M. O'Neill, R. J. Ford, R. Palanivel, M. O'Brien, et al. 2013. Single phosphorylation sites in Acc1 and Acc2 regulate lipid homeostasis and the insulin-sensitizing effects of metformin. *Nat. Med.* **19:** 1649–1654.
37. Davies, S. P., D. Carling, M. R. Munday, and D. G. Hardie. 1992. Diurnal rhythm of phosphorylation of rat liver acetyl-CoA carboxylase by the AMP-activated protein kinase, demonstrated using freeze-clamping. Effects of high fat diets. *Eur. J. Biochem.* **203:** 615–623.
38. Hawley, S. A., M. D. Fullerton, F. A. Ross, J. D. Schertzer, C. Chevtzoff, K. J. Walker, M. W. Peggie, D. Zibrova, K. A. Green, K. J. Mustard, et al. 2012. The ancient drug salicylate directly activates AMP-activated protein kinase. *Science.* **336:** 918–922.
39. Beyea, M. M., C. L. Heslop, C. G. Sawyez, J. Y. Edwards, J. G. Markle, R. A. Hegele, and M. W. Huff. 2007. Selective up-regulation of LXR-regulated genes ABCA1, ABCG1, and APOE in macrophages through increased endogenous synthesis of 24(S),25-epoxycholesterol. *J. Biol. Chem.* **282:** 5207–5216.
40. Rowe, A. H., C. A. Argmann, J. Y. Edwards, C. G. Sawyez, O. H. Morand, R. A. Hegele, and M. W. Huff. 2003. Enhanced synthesis of the oxysterol 24(S),25-epoxycholesterol in macrophages by inhibitors of 2,3-oxidosqualene:lanosterol cyclase: a novel mechanism for the attenuation of foam cell formation. *Circ. Res.* **93:** 717–725.
41. Galic, S., M. D. Fullerton, J. D. Schertzer, S. Sikkema, K. Marcinko, C. R. Walkley, D. Izon, J. Honeyman, Z. P. Chen, B. J. van Denderen, et al. 2011. Hematopoietic AMPK beta1 reduces mouse adipose tissue macrophage inflammation and insulin resistance in obesity. *J. Clin. Invest.* **121:** 4903–4915.
42. Thaiss, C. A., S. Itav, D. Rothschild, M. Meijer, M. Levy, C. Moresi, L. Dohnalova, S. Braverman, S. Rozin, S. Malitsky, et al. 2016.

Persistent microbiome alterations modulate the rate of post-dieting weight regain. *Nature.* **540:** 544–551.
43. Wu, X., M. Song, M. Wang, J. Zheng, Z. Gao, F. Xu, G. Zhang, and H. Xiao. 2015. Chemopreventive effects of nobiletin and its colonic metabolites on colon carcinogenesis. *Mol. Nutr. Food Res.* **59:** 2383–2394.
44. Koga, N., C. Ohta, Y. Kato, K. Haraguchi, T. Endo, K. Ogawa, H. Ohta, and M. Yano. 2011. In vitro metabolism of nobiletin, a polymethoxy-flavonoid, by human liver microsomes and cytochrome P450. *Xenobiotica.* **41:** 927–933.
45. Pinkosky, S. L., R. S. Newton, E. A. Day, R. J. Ford, S. Lhotak, R. C. Austin, C. M. Birch, B. K. Smith, S. Filippov, P. H. E. Groot, et al. 2016. Liver-specific ATP-citrate lyase inhibition by bempedoic acid decreases LDL-C and attenuates atherosclerosis. *Nat. Commun.* **7:** 13457.
46. Smith, B. K., R. J. Ford, E. M. Desjardins, A. E. Green, M. C. Hughes, V. P. Houde, E. A. Day, K. Marcinko, J. D. Crane, E. P. Mottillo, et al. 2016. Salsalate (Salicylate) uncouples mitochondria, improves glucose homeostasis, and reduces liver lipids independent of AMPK-beta1. *Diabetes.* **65:** 3352–3361.
47. Lindholm, C. R., R. L. Ertel, J. D. Bauwens, E. G. Schmuck, J. D. Mulligan, and K. W. Saupe. 2013. A high-fat diet decreases AMPK activity in multiple tissues in the absence of hyperglycemia or systemic inflammation in rats. *J. Physiol. Biochem.* **69:** 165–175.
48. Lowell, B. B., V. S-Susulic, A. Hamann, J. A. Lawitts, J. Himms-Hagen, B. B. Boyer, L. P. Kozak, and J. S. Flier. 1993. Development of obesity in transgenic mice after genetic ablation of brown adipose tissue. *Nature.* **366:** 740–742.
49. Ruderman, N. B., D. Carling, M. Prentki, and J. M. Cacicedo. 2013. AMPK, insulin resistance, and the metabolic syndrome. *J. Clin. Invest.* **123:** 2764–2772.
50. Lee, Y. S., B. Y. Cha, K. Saito, H. Yamakawa, S. S. Choi, K. Yamaguchi, T. Yonezawa, T. Teruya, K. Nagai, and J. T. Woo. 2010. Nobiletin improves hyperglycemia and insulin resistance in obese diabetic ob/ob mice. *Biochem. Pharmacol.* **79:** 1674–1683.
51. He, B., K. Nohara, N. Park, Y. S. Park, B. Guillory, Z. Zhao, J. M. Garcia, N. Koike, C. C. Lee, J. S. Takahashi, et al. 2016. The small molecule nobiletin targets the molecular oscillator to enhance circadian rhythms and protect against metabolic syndrome. *Cell Metab.* **23:** 610–621.
52. Nohara, K., V. Mallampalli, T. Nemkov, M. Wirianto, J. Yang, Y. Ye, Y. Sun, L. Han, K. A. Esser, E. Mileykovskaya, et al. 2019. Nobiletin fortifies mitochondrial respiration in skeletal muscle to promote healthy aging against metabolic challenge. *Nat. Commun.* **10:** 3923.
53. Eguchi, A., A. Murakami, S. Li, C. T. Ho, and H. Ohigashi. 2007. Suppressive effects of demethylated metabolites of nobiletin on phorbol ester-induced expression of scavenger receptor genes in THP-1 human monocytic cells. *Biofactors.* **31:** 107–116.
54. Li, S., S. Sang, M. H. Pan, C. S. Lai, C. Y. Lo, C. S. Yang, and C. T. Ho. 2007. Anti-inflammatory property of the urinary metabolites of nobiletin in mouse. *Bioorg. Med. Chem. Lett.* **17:** 5177–5181.
55. Wu, X., M. Song, K. Rakariyatham, J. Zheng, S. Guo, Z. Tang, S. Zhou, and H. Xiao. 2015. Anti-inflammatory effects of 4′-demethylnobiletin, a major metabolite of nobiletin. *J. Funct. Foods.* **19:** 278–287.